Atmos. Chem. Phys. Discuss., 11, 17825–17877, 2011
www.atmos-chem-phys-discuss.net/11/17825/2011/
doi:10.5194/acpd-11-17825-2011


Atmospheric Chemistry and Physics Discussions



# Variable lifetimes and loss mechanisms for $NO_3$ and $N_2O_5$ during the DOMINO campaign: contrasts between marine, urban and continental air

**J. N. Crowley[1], J. Thieser[1], M. Tang[1], G. Schuster[1], H. Bozem[1], Z. Hosaynali Beygi[1], H. Fischer[1], J. Diesch[2], F. Drewnick[2], S. Borrmann[2,3], W. Song[1], N. Yassaa[1,4], J. Williams[1], D. Pöhler[5], U. Platt[5], and J. Lelieveld[1]**

[1]Max-Planck-Institut für Chemie, Division of Atmospheric Chemistry, Mainz, Germany
[2]Max-Planck-Institut für Chemie, Particle Chemistry Department, Mainz, Germany
[3]Institute for Atmospheric Physics, University of Mainz, Mainz, Germany
[4]Faculty of Chemistry, University of Sciences and Technology Houari Boumediene (USTHB), Algiers, Algeria
[5]Institut of Environmental Physics, University of Heidelberg, Heidelberg, Germany

Received: 8 June 2011 – Accepted: 10 June 2011 – Published: 23 June 2011

Correspondence to: J. N. Crowley (john.crowley@mpic.de)

Published by Copernicus Publications on behalf of the European Geosciences Union.







## Abstract

Nighttime mixing ratios of boundary layer $N_2O_5$ were determined using cavity-ring-down spectroscopy during the DOMINO campaign. Observation of $N_2O_5$ was intermittent, with mixing ratios ranging from below the detection limit (~5 ppt) to ~500 ppt. A steady-state analysis constrained by measured mixing ratios of $NO_2$ and $O_3$ was used to derive $NO_3$ lifetimes and compare them to calculated rates of loss via gas-phase and heterogeneous reactions of both $NO_3$ and $N_2O_5$. Three distinct types of air masses were encountered, which were largely marine (Atlantic), continental or urban-industrial in origin. $NO_3$ lifetimes were longest in the Atlantic sector (up to ~30 min) but were very short (a few seconds) in polluted, air masses from the local city and petroleum-related industrial complex of Huelva. Air from the continental sector was an intermediate case. The high reactivity to $NO_3$ of the urban air mass was not accounted for by gas-phase and heterogeneous reactions, rates of which were constrained by measurements of NO, volatile organic species and aerosol surface area. In general, high $NO_2$ mixing ratios resulted in low $NO_3$ lifetimes, though heterogeneous processes (e.g. reaction of $N_2O_5$ on aerosol) were generally less important than direct gas-phase losses of $NO_3$. The presence of $SO_2$ at levels above ~2 ppb in the urban air sector was always associated with very low $N_2O_5$ mixing ratios indicating either very short $NO_3$ lifetimes in the presence of combustion-related emissions or an important role for reduced sulphur species in urban, nighttime chemistry. High production rates coupled with low lifetimes of $NO_3$ imply an important contribution of nighttime chemistry to removal of both $NO_x$ and VOC.

## 1 Introduction

The photochemically driven, OH-initiated oxidation processes during the day are supplemented by (or, for several classes of volatile organic compounds (VOCs) such as terpenes or $CH_3SCH_3$, surpassed by) night-time reactions with the $NO_3$ radical (Wayne





ACPD
11, 17825–17877, 2011



et al., 1991). The interaction of $NO_3$ with VOCs leads to the formation of organic peroxy radicals, $HO_2$ and OH via reactions of $HO_2$ with $O_3$ or $NO_3$. $NO_3$ can thus initiate and propagate nocturnal radical chemistry (Platt et al., 1990; Sommariva et al., 2009) linking $HO_2$ and $NO_x$ chemistry and significantly impacting on oxidation rates of several classes of atmospheric traces gases.

$NO_3$ is formed predominantly in the reaction of $NO_2$ with ozone (Reaction R1) and is converted to $N_2O_5$ via further reaction with $NO_2$ (Reaction R2). The thermal decomposition of $N_2O_5$ links the concentrations of $NO_3$ and $N_2O_5$ via the equilibrium constant, $K_2$. Simultaneous measurements of $NO_3$ and $N_2O_5$ (Brown et al., 2003a; Crowley et al., 2010) confirm that (under most conditions) the timescales to acquire equilibrium are sufficiently short that the relative concentrations of $NO_3$ and $N_2O_5$ in the atmosphere are controlled only by the temperature and levels of $NO_2$.

$$NO_2 + O_3 \rightarrow NO_3 + O_2 \quad \text{(R1)}$$

$$NO_2 + NO_3 + M \rightarrow N_2O_5 + M \quad \text{(R2a)}$$

$$N_2O_5 + M \rightarrow NO_2 + NO_3 + M \quad \text{(R2b)}$$

The production rate of $NO_3$ is given by $k_1[NO_2][O_3]$ (generally we write $k_i$ as the rate coefficient for Reaction Ri) so that its stationary state turnover lifetime, $\tau_{ss}(NO_3)$, can be calculated from observations of its concentration and those of $O_3$ and $NO_2$:

$$\tau_{ss}(NO_3) = \frac{[NO_3]}{k_1[NO_2][O_3]} \quad (1)$$

Whenever we use the term "$NO_3$ lifetimes" in the manuscript, we refer to $\tau_{ss}(NO_3)$.

$NO_3$ can be removed directly from the air by e.g. reaction with organic trace gases (Wayne et al., 1991) or indirectly via removal of $N_2O_5$ via e.g. heterogeneous loss to aqueous particles. As described previously (Geyer et al., 2001b; Aldener et al., 2006; Crowley et al., 2010) the contributions of direct and indirect losses of $NO_3$ to its lifetime





ACPD
11, 17825–17877, 2011



can, in principal, be evaluated if $K_2$ (the equilibrium constant $k_2/k_{-2}$) and [$NO_2$] are known:

$$\tau_{ss}(NO_3) \approx \frac{1}{f_{ss}(NO_3)} \quad (2)$$

where $f_{ss}(NO_3)$ is the overall loss frequency of $NO_3$ from stationary state and is equal to

$$\Sigma_i (k_i [X]_i) + 0.25\,\bar{c}\gamma(NO_3)A + f_{dd}(NO_3) + \left(0.25\,\bar{c}\gamma(N_2O_5)A + f_{dd}(N_2O_5) + f_{H_2O}\right) K_2 [NO_2]$$

In this expression, $k_i$ ($cm^3$ molecule$^{-1}$ $s^{-1}$) is the rate coefficient for reaction of $NO_3$ with trace gas i at concentration $[X]_i$ (molecule $cm^{-3}$), $A$ is the aerosol surface area density ($cm^2$ $cm^{-3}$), $\bar{c}$ (cm $s^{-1}$) is the mean molecular velocity of $NO_3$ or $N_2O_5$, $\gamma(NO_3)$ and $\gamma(N_2O_5)$ are the dimensionless uptake coefficients for irreversible reaction of $NO_3$ or $N_2O_5$ with aerosol, $f_{dd}(s^{-1})$ is the first-order rate constant for dry deposition of $NO_3$ or $N_2O_5$ and $f_{H_2O}$ ($s^{-1}$) represents the homogeneous, gas-phase loss of $N_2O_5$ via reaction with water vapour.

Recent measurements of long lifetimes of $N_2O_5$ even in the presence of high relative humidity (Brown et al., 2009; Crowley et al., 2010) imply that $f_{H_2O}$ is too small to be important under most conditions. In contrast, the heterogeneous hydrolysis of $N_2O_5$ on or in sulphate aerosol has been well established in field and laboratory experiments (see below) and can substantially modify the amount of reactive nitrogen available for daytime photochemical $O_3$ production. In the polluted boundary layer, this process influences the fate of $NO_x$ emissions and their potential for photochemical ozone formation and also (via heterogeneous chemistry on sulphate particles) links $O_3$ production rates to emissions of $SO_2$ from e.g. power plants or shipping (Brown et al., 2006).

The rate of uptake of a trace gas to airborne particles can be reduced by concentration gradients close to the particle surface, which requires modification of the simple expression for the heterogeneous loss rate, $k_{het} = 0.25\,\bar{c}\gamma A$, as used in Eq. (2). The





ACPD
11, 17825–17877, 2011



effective uptake coefficient ($\gamma_{\text{effective}}$) is approximated by (Fuchs and Sutugin, 1970):

$$\frac{1}{\gamma_{\text{effective}}} = \frac{1}{\gamma} + \frac{0.75 + 0.283\,Kn}{Kn(Kn+1))} \quad (3)$$

where $Kn = \frac{3D_g}{\bar{c} \cdot r_{sw}}$, $r_{sw}$ is the radius of the particle at the maximum of the surface area weighted size distribution, and $D_g$ is the gas phase diffusion coefficient of $N_2O_5$ or $NO_3$ at the appropriate pressure and temperature. For $N_2O_5$, $D_g$ is 0.085 $cm^2\,s^{-1}$ at atmospheric pressure and 298 K (Wagner et al., 2008). During the nights of the campaign, the dominant contribution to aerosol surface area was by particles with diameters of less than 100 nm. In this case, only uptake coefficients close to unity require significant correction. For example, an uptake coefficient of ~0.1 would be reduced by transport limitations to ~0.09, whereas a $\gamma$ of 1 would reduce to 0.5. A value of 0.5 is therefore the approximate maximum value of $\gamma$ ($N_2O_5$) or $\gamma$ ($NO_3$), which can reasonably be used to calculate $NO_3$ lifetimes using Eq. (2). More realistic (lower) values of $\gamma$, derived from laboratory and field experiments are discussed later.

At low aerosol loading (or low values of $\gamma$) and negligible dry deposition the right-hand term in the denominator of Eq. (2) becomes diminishingly small and $NO_3$ lifetimes are largely independent of $NO_2$ concentrations. On the other hand, if gas-phase losses of $NO_3$ are slow, $N_2O_5$ chemistry can be important and $NO_3$ lifetimes will show a dependence on the inverse $NO_2$ concentration (Heintz et al., 1996; Martinez et al., 2000; Geyer et al., 2001b; Brown et al., 2003a, b, 2009; Aldener et al., 2006).

Certain conditions must be fulfilled if Eq. (2) is used to examine $NO_3$ lifetimes and draw conclusions regarding direct and indirect loss routes. Firstly, $NO_3$ production rates are governed by a slow reaction between $NO_2$ and $O_3$. Application of a stationary state analysis to $NO_3$ lifetimes is only suited to air-masses where the chemical lifetime of $NO_3$ (or $N_2O_5$) is sufficiently short that stationary state is achieved with the transport time from the emission region to the measurement site (Brown et al., 2003a).

Stationary state is formally achieved when the rate of change of $NO_3$ and $N_2O_5$ are zero, i.e. $dNO_3/dt = k_1[NO_2][O_3] + k_{-2}[N_2O_5] - k_2[NO_2][O_3] - k'(NO_3)[NO_3] = 0$ and





ACPD
11, 17825–17877, 2011



$d[N_2O_5]/dt = k_2[NO_2][NO_3] - k_{-2}[N_2O_5] - k''[N_2O_5] = 0$, where $k'(NO_3)$ and $k''(N_2O_5)$ are first order loss rate constants for any reactions involving $NO_3$ and $N_2O_5$. The approximate time to achieve stationary state thus depends on the production and loss rates of both $NO_3$ and $N_2O_5$ and is longer at high $NO_2$ mixing ratio and low temperatures.

Time dependent values of $d[NO_3]/dt$ and $d[N_2O_5]/dt$ were determined for an unfavourable case (i.e. high $NO_2$ mixing ratio of 10 ppb) by numerical simulation in a manner similar to that described previously (Brown et al., 2003a). Input parameters to the simulations were the measured $NO_2$ and $O_3$ concentrations and temperature dependent kinetic expressions for Reactions (R1) and (R2) (together defining the production rates of $NO_3$ and $N_2O_5$). Values for $k'$ and $k''$ were adjusted so that simulated $NO_3$ and $N_2O_5$ mixing ratios were similar to those measured. The low $N_2O_5$ and $NO_3$ concentrations observed (implying short lifetimes) meant that stationary state was achieved within 1–2 h after dusk and within the time of transport from the major source of $NO_x$ (e.g. Huelva).

Expression Eq. (2) has been used to derive the direct and indirect contributions to $NO_3$ loss rates (Brown et al., 2009; Crowley et al., 2010) via the dependence of the observed lifetime on $NO_2$ mixing ratios. This approach will however break down if the trace gases which react directly with $NO_3$ are correlated (e.g. have the same chemical source or spatial distribution of emissions) with $NO_2$. This is unlikely to apply to regions where $NO_3$ losses are dominated by e.g. reaction with biogenic volatile organic compounds (BVOC) in clean air masses, but might be the case where $NO_3$ reacts with traces gases resulting from combustion processes in which $NO_2$ is also generated. In a similar vein, if aerosol surface area also co-varies with $NO_2$, use of Eq. (2) to separate the contributions of homogeneous and heterogeneous loss rates of $N_2O_5$ to the $NO_3$ lifetime is not possible.





ACPD
11, 17825–17877, 2011



## 2 Site description

The DOMINO campaign (Diel Oxidant Mechanisms In relation to Nitrogen Oxides, (21 November 2008–8 December 2008) took place at the Atmospheric Sounding Station (Base de Arenosillo[1], 37°05′58″ N, 6°44′17″ W) located on the Atlantic coast of the southern Spanish region of Moguer (Fig. 1). Measurements were conducted in a forested area (mainly Stone pines, *Pinus pinea* ∼5–10 m in height) with proximity to both extensive pollution sources and the Atlantic Ocean (the Atlantic coast was ∼300 m distant and ∼20 m lower) so that the chemical composition of air masses arriving at the site was highly dependent on wind direction. On-site wind directions between 290 and 340 degrees indicated that air masses had recently passed over the expansive industrial centre and port of Huelva (henceforth referred to as the "Huelva" sector) which was located about 30 km away, or with typical night-time wind-speeds of 8–18 km/h about 2–3 h upwind. Huelva houses one of Europe's larger oil refineries and pollution from this sector includes emissions from related industrial/shipping activity. Air from the Huelva sector arriving at the measurement site at night was frequently and strongly malodorous. Air arriving from the 150–270 degrees sector passed over the Atlantic (sector "Atlantic") and generally contained low levels of $NO_x$. $NO_2$ plumes were occasionally observed in this sector, which were usually accompanied by enhanced levels of $SO_2$ indicating emissions from passing ships.

Wind directions between 0 and 45 degrees (sector "continental") were from mainland Spain and passed no large cities for several hours prior to arrival at the site. Air arriving from Sevilla (∼60 degrees), following Huelva, the next largest potential source of pollutants, was rarely encountered during the night. Overall, during the nights of the campaign, the air arrived predominantly from the Huelva (∼50 %) or continental sectors (∼35 %), with air from the Atlantic sector (∼15%) encountered less frequently.

[1]El Arenosillo is a platform of the Atmospheric Research and Instrumentation Branch of the Spanish National Institute for Aerospace Technology (INTA) dedicated to atmospheric measurements in the Southwest of Spain.





ACPD
11, 17825–17877, 2011



Air mass back-trajectories calculated using HYSPLIT with GDAS meteorology (Draxler and Rolph, 2011) confirmed the allocation of source region sector according to local wind directions. Figure 1 displays selected back-trajectories or air arriving at midnight from the Huelva sector (1), the continental sector (2) and the Atlantic sector (3).

## 3 Methods

### 3.1 $NO_3$ and $N_2O_5$

$NO_3$ and $N_2O_5$ mixing ratios were measured using a two-channel, off axis cavity-ring-down system (OA-CRD), which has recently been described in detail (Schuster et al., 2009; Crowley et al., 2010). and also by long-path, differential optical absorption spectroscopy (LP-DOAS). In the CRD instrument, one channel monitors $NO_3$ directly, the other is used to monitor the sum of $NO_3$ and $N_2O_5$ via thermal dissociation of $N_2O_5$. The instrument was located in the upper container of a two-container stack and sampled air through a few meters of 1/4 or 1/2″ PFA-tubing with the inlet sampling from a height of between 7 and 12 m above ground level (~1–5 m above the closest canopy).

The 1/2″ inlet was operated with a large bypass flow to reduce the residence time. A 2 µm pore Teflon filter (replaced every hour) in a PFA filter holder was located at the end of the inlet outside the container. The losses of $NO_3$ and $N_2O_5$ to the filter were characterised prior to and after the campaign. Loss rates in the cavities were also measured during the campaign. Operational pressures and flows resulted in residence times in the inlet lines and cavities of between 0.6 and 1 s. CRD noise-levels changed during the campaign and varied between ~3 and 7 pptv for $N_2O_5$ and between 2 and 5 pptv for $NO_3$ (both with 5 s integration per datapoint). The detection limit is partly defined by accuracy of the chemical zero (measured by adding NO as described in detail previously (Schuster et al., 2009)) and was between 2 and 3 pptv for $NO_3$ and 5–7 pptv for $N_2O_5$. $NO_3$ was not observed directly during the campaign even when $N_2O_5$ levels of several hundred pptv were present. As $NO_2$ levels were not sufficiently high and





ACPD
11, 17825–17877, 2011



temperatures (controlling $K_2$) not sufficiently low to reduce $NO_3$ to below the detection limit, this indicates deviation of the $NO_2$-$NO_3$-$N_2O_5$ chemistry from equilibrium. With night-time temperatures occasionally as high as 15 °C, equilibrium should be established within in a few minutes, suggesting that any processes that rapidly drain $NO_3$ from equilibrium must be very local otherwise $N_2O_5$ would also have been completely removed.

Total loss of $NO_3$ in the PFA inlet had not been anticipated as this had not been encountered on a previous campaign at a rural location (Crowley et al., 2010) in which a similar sampling strategy had been deployed. Use of new inlet lines did not result in observation of $NO_3$, even temporarily. On several occasions during the campaign a calibration source of $NO_3$ was added to the inlet to measure its transmission and also that of the $NO_3$ cavity. $NO_3$ was generated by the thermal decomposition (~90 °C) of $N_2O_5$, itself made by mixing $NO_2$ and $O_3$ in a blackened, FEP-coated glass reaction vessel as described previously (Schuster et al., 2009). Prior to heating, the mixture typically contained approximately 200–400 pptv $N_2O_5$, 150 ppbv $O_3$ and 5 ppbv $NO_2$. The results were rather surprising as the initial transmission of the inlet tubing to $NO_3$ was very low (on occasions less than 20 %) even if it was relatively fresh. The transmission increased with exposure to the $O_3$, $NO_2$, $NO_3$ mixture to a value (circa 70–80 %) commensurate with known loss rates of $NO_3$ in PFA tubing. This condition sometimes took as long as an hour to achieve. At the same time, loss rates of $NO_3$ in the cold cavity were recorded as high as 1 $s^{-1}$, a factor 5 larger than observed in the laboratory, whereas loss in the hot cavity (i.e. the $N_2O_5$ + $NO_3$ channel) proceeded at the usual rate (~0.2 $s^{-1}$). These observations indicate that the PFA tubing rapidly became reactive to $NO_3$ when exposed to the air and this reactivity could be reduced by extended passivation with high $NO_3/O_3$ concentrations or by heating to 90 °C.

Assuming that the loss of $NO_3$ occurred in our inlet, it took place on a timescale (1 s) which is considerably shorter than the thermal lifetime of $N_2O_5$ (minutes), so that the $N_2O_5$ mixing ratios would not have been significantly affected. In this case we can calculate $NO_3$ ambient mixing ratios from the measured $N_2O_5$ and $NO_2$ and the





ACPD
11, 17825–17877, 2011



equilibrium constant, $K_2$ via Eq. (4).

$$[NO_3] = \frac{[N_2O_5]}{K_2[NO_2]} \quad (4)$$

As the inlet tubing was protected with a Teflon filter we do not anticipate large losses of $N_2O_5$ due to coating of the wall with aerosol. The disadvantage with this indirect calculation of $NO_3$ is that it relies on high quality (accurate, low noise), and preferably high time resolution $NO_2$ measurements. Some uncertainty is also associated with $K_2$, though recent field measurements of $NO_2$, $NO_3$ and $N_2O_5$ suggest that this is not more than 20 % (Osthoff et al., 2007; Crowley et al., 2010). The uncertainty in $NO_3$ mixing ratios calculated this way is thus considerably larger than via direct measurements and are estimated as about 35 % if $N_2O_5$<7 ppt. At lower levels of $N_2O_5$ the uncertainty in $N_2O_5$ (~40 % at 5 ppt) dominates. Long-path diferential optical absorption spectroscopy (LP-DOAS, see below) measurements of $NO_3$ taken at a similar height to the CRD inlet are however in good agreement with the CRD-$NO_3$ mixing ratios derived from $N_2O_5$ and $NO_2$.

The LP-DOAS instrument applies the setup from (Merten et al., 2011) with a configuration explained in (Pöhler et al., 2010). It uses a telescope of 1.5 m focal length a 100 or 200 µm fibre bundle a 75W XBO xenon arc lamp (Osram) and for spectral analysis an Acton 300i spectrometer with Roper Scientific CCD camera (Spec-10:2KBUV). The instrument was located at 9m above the ground about 800 m north of the main sampling point. It was operated with three sets of retro-reflectors mounted on a tower at 20, 35 and 70 m above the ground at a distance of 4.8 km to the east, resulting in a total optical path-length of 9.6 km. The data analysis of $NO_3$ was performed in the spectral range from 615.0 nm to 673.8 nm with a gap between 644.1 nm to 657.8 nm to avoid strong water absorption lines. The reference spectra used were: $NO_3$ (Yokelson et al., 1994), $NO_2$ (Vandaele et al., 1998), $O_3$ (Voigt et al., 2001), $H_2O$ (Hitran, 2006, from Gordon et al., 2007) and additionally a spectrum recorded at noon to correct for most $H_2O$ absorption, a background spectrum and a 3rd order polynomial. The





ACPD
11, 17825–17877, 2011



standard deviation $\sigma$ of the measurements was estimated according to Stutz and Platt (Stutz and Platt, 1996) and resulted in an average uncertainty for the $NO_3$ mixing ratio of 1 ppt. In this work we use data at from the lowest retro-reflector only in order to compare with the CRD measurements.

### 3.2 $NO_2$ and NO

NO and $NO_2$ measurements were made with a modified commercial chemiluminescence detector (CLD 790 SR) originally manufactured by ECO Physics (Duernten, Switzerland). The quantitative detection of $NO_2$ is based on its photolytic conversion (Blue Light Converter, Droplet Measurement Technologies, Boulder, CO, USA) to NO, which was subsequently detected in the CLD (Kley and McFarland, 1980). The detection limits for the NO and $NO_2$ measurements were 6 pptv and 8 ppt, respectively for an integration period of 1s. The total uncertainties for the measurements of NO, $NO_2$ were determined both to be 10 %, based on the reproducibility of in-field background measurements, calibrations, the uncertainties of the standards and the conversion efficiency of the photolytic converter. The same device was described in more detail recently (Crowley et al., 2010).

### 3.3 $O_3$, $SO_2$ and $H_2O$

$O_3$ and $SO_2$ (Airpointer, Recordum GmbH) and $H_2O$ (LICOR 840 gas analyser, LI-COR, Inc.) were measured using instrumentation onboard the MoLa mobile platform (Diesch et al., 2011). Limits of detection and precision were 0.5 ppb and 1 ppb for both $SO_2$ and $O_3$, 0.4 ppb and 1 ppb for $NO_x$. Whilst Airpointer measurements of NO and $NO_2$ mirrored the trends seen using the ECO Physics device described above, they were not sufficiently accurate (especially at low $NO_x$ levels) to perform $NO_3$ lifetime analyses.





ACPD
11, 17825–17877, 2011



### 3.4 Volatile organic compounds

A commercially available instrument (AERO Laser model AL 4021, Germany) was used for in-situ HCHO measurements. This instrument is based on the Hantzsch reagent method, following the design described in Kelly and Fortune (1994). The time resolution is 160 sec. Detection limit and precision were estimated from the $1\sigma$-reproducibility of in-situ zero and calibration gas measurements as 22 pptv and ±15 %, respectively. The total uncertainty is estimated to be 29 %. An on-line sampling TD-GC-MSD measurement system was used for the in-situ observation of anthropogenic VOCs such as ethylbenzene, and all xylene isomers as well as biogenic species such as isoprene and monoterpenes (Song et al., 2011). $C_1$-$C_4$ alkenes and alkanes were not measured.

### 3.5 Aerosol measurements

Particle size information was obtained using MoLa instruments (see above). A Fast Mobility Particle Sizer (FMPS 3091, TSI, Inc.), an Aerodynamic Particle Sizer (APS 3321, TSI, Inc.) as well as an Optical Particle Counter (OPC 1.109, Grimm) covered a particle size range from 5.6 nm to 32 µm. The chemical composition of the non-refractory aerosol in the sub-micron range was measured by means of a High-Resolution-Time-of-Flight Aerosol Mass Spectrometer (HR-ToF-AMS, Aerodyne Res., Inc.). The soot (black carbon) concentration in $PM_1$ was determined by a Multi Angle Absorption Photometer (MAAP, Thermo E.C.). The aerosol surface area (ASA) used for calculating rates of trace gas uptake was calculated only from the FMPS dataset as, for most nights (including those examined in detail later), this contributed ≥80 % of the total aerosol surface area and (in contrast to super-micron particles) was of known composition.





ACPD
11, 17825–17877, 2011



### 3.6 Meteorological parameters

Wind direction and speed, temperature and pressure and relative humidity and rain intensity at approximate inlet height were provided by MoLa instrumentation (WXT 510 weather station, Vaisala). Temperatures and wind directions were also available at heights of 25, 50 and 100 m from a local meteorological tower operated by INTA.

Several cloudless nights gave rise to a strong temperature inversion, with temperatures at a height of 100 m up to 5–6 °C warmer than those measured at the inlet height (~10 m). This inversion would have lead to a very stable nocturnal boundary layer with efficient accumulation of low altitude emissions from e.g. the Huelva industrial area.

## 4 Measurements and discussion

Measurements of $N_2O_5$ and $NO_3$ were made on all campaign nights with the exception of 28 November. $N_2O_5$ was observed on most nights, though it was never present above the detection limit throughout the night but rather appeared in bursts of a few hours duration, reflecting differences in production and loss rates with changes in air-mass origin and/or local emissions. The observed mixing ratios of $N_2O_5$ are plotted for each night of the campaign in Fig. 2. As described above, $NO_3$ could not be detected directly using CRD but its mixing ratio was calculated from those of $N_2O_5$ and $NO_2$ and the equilibrium constant, $K_2$. The $NO_3$ data are generally in good agreement with DOAS measurements considereing the differences in location and heights of inlet (CRD) and optical path (LP-DOAS).

As shown in Reactions (R1)–(R2), the production rates of $NO_3$ and $N_2O_5$ are governed by the $NO_2$ and $O_3$ mixing ratios. During the DOMINO campaign, night-time mixing ratios of $NO_2$ were highly variable, fluctuating from local background levels of ~1 ppbv to more than 15 ppb. The highest levels of $NO_2$ were associated with air masses that had passed over the Huelva sector, often arriving in plumes with a duration of about 1–2 h. Sub-ppbv levels of $NO_2$ were usually associated with the Atlantic





ACPD
11, 17825–17877, 2011



sector. Apart from infrequent NO spikes presumably from traffic using local roads, night-time levels of NO were low. They were however, occasionally non-zero and on some nights 5–10 pptv of NO was present for a prolonged duration. Given that the lifetime of NO in the presence of >15 ppbv $O_3$ is only a few minutes, the presence of NO implies a local source. Indeed, with an average night-time wind-speeds of just 2.8 m/s this implies a source located within about 500 m of the inlet. Possible sources of NO are emissions from the surrounding woodland soil or contamination via the common exhaust lines used by the various measurements. Apart from occasional plumes from Huelva, non-zero levels of NO were not associated with any single wind-direction which argues against a local, continuous point emission source (i.e. our instrument exhaust-lines).

Night-time $O_3$ was strongly anti-correlated with $NO_2$ and thus also showed significant variability, with typical levels of 15–40 ppbv. Air masses passing over the Huelva and coastal region (and sometimes the open ocean) often contained $SO_2$, with maximum levels of ~40 ppbv in plumes originating from the port or Huelva areas. The $SO_2$ plumes were always associated with high levels of $NO_2$ with a similar temporal profile, indicating a common process as source. This might have been the result of petrochemical industry activity as flaring at the petrochemical complex in Huelva was frequently visible at night. A further possible source of $SO_2$ was ship emissions, either at sea or entering the harbour at Huelva. Note that the strait of Gibraltar (~160 km distant) is one of the world's busiest shipping lanes. $SO_2$ was not observed above the limit of detection from the continental sector. We note that the presence of both $SO_2$ and $NO_2$ in a plume nearly always meant low levels or non-detection of $N_2O_5$, despite high $NO_3$ production rates. We discuss this particular aspect of $NO_3/N_2O_5$ chemistry in more detail later when analysing individual days.

Particles measured at the site displayed number size distributions with mode diameters of between 40 and 80 nm with a generally dominant organic fraction but with a significant sulphate component with short term increases that correlated with $SO_2$ plumes. The ammonium to sulphate mole ratio was always less than unity during the





ACPD
11, 17825–17877, 2011



campaign, indicating that the aerosol was acidic (ratio of 2 = neutral aerosol).

### 4.1 $NO_3$ lifetimes

Despite large $NO_3$ production rates $N_2O_5$ and thus $NO_3$ were only sporadically observed, indicating reactive air-masses and short $NO_3$ or $N_2O_5$ lifetimes. More than 50 % of the campaign data revealed $NO_3$ lifetimes of less than 1 min, with lifetimes longer than 15 min representing only 0.5 % of the measurements. $NO_3$ lifetimes were found to be strongly dependent on wind direction, with the largest values measured in air masses originating from the Atlantic sector and the shortest lifetimes when air arrived from Huelva, with continental air an intermediate case. This is illustrated in Fig. 3.

During the campaign, $NO_3$ lifetimes were seen to be reduced at high $NO_2$ mixing ratios. Frequently, this is taken to be indicative of indirect losses of $NO_3$ (i.e. $N_2O_5$ driven, heterogeneous reactions). However, the $NO_2$ mixing ratio was also correlated with the available surface area, so that separation of the $NO_3$ losses into direct and indirect reactions (see Eq. 2) is problematic.

Below, we consider $NO_3$ lifetimes on three nights of the campaign in some detail, attempting to identify and quantify the various direct and indirect processes controlling $NO_3$ lifetimes. Each day represents a different air mass origin, covering each of the Atlantic, Huelva and continental sectors.

#### 4.1.1 6–7 December: clean air from the Atlantic sector

Local wind directions indicated that air masses encountered during the latter part of the night spanning 6–7 December arrived from the Atlantic sector. Back trajectories (Fig. 1) confirmed that the air had spend at least 3 days over the Atlantic Ocean prior to arriving at the site.

Selected trace gas and aerosol measurements, meteorological data and calculated $NO_3$ lifetimes are plotted in Fig. 4. After 02:30, $O_3$ levels were between 25 and 35 ppb,





ACPD
11, 17825–17877, 2011



with $NO_2$ close to 1 ppbv, resulting in comparatively low $NO_3$ production rates. On this night, $NO_3$ and $N_2O_5$ measurements started only at 01:45 on 7 December due to instrument tests. $N_2O_5$ was observed at levels up to ~50 pptv with $NO_3$ lifetimes (calculated via Eq. 1) occasionally greater than 30 min. These represent the longest $NO_3$ lifetimes encountered during the campaign and are consistent with observations of extended $NO_3$ lifetimes in marine air at low $NO_x$ mixing ratios (Heintz et al., 1996; Carslaw et al., 1997a, b; Allan et al., 2000). The CRD (calculated) and LP-DOAS derived $NO_3$ mixing ratios were in good agreement for most of the night. $N_2O_5$ was, however, not observed before ~02:30 and its calculated lifetime was less than ~100 s prior to this time. Similarly, $NO_3$ lifetimes decreased more or less constantly from 04:30 until dawn. In both cases the short $NO_3$ lifetime was accompanied by non-zero NO mixing ratios and enhanced $NO_2$ levels. Prior to 02:30 somewhat reduced $O_3$ mixing ratios were observed along with elevated levels of $SO_2$ (2-3 ppbv) and a ~20 pptv spike in the NO mixing ratio at 02:00, indicating some influence of local emissions. A rough estimate (ignoring dilution) of the age of the NO/$NO_2$ plume of ~350 s could be estimated from the enhancement in the $NO_2$ mixing ratio (~700 pptv), the NO and $O_3$ mixing ratios and rate constant for Reaction (R1). The observation of a decrease in a biogenic trace gas (pinene) from 10–20 pptv before 02:30 to 2-3 pptv after 02:30 supports a change in air-mass origin at this time.

Also apparent are three rapid increases in the $N_2O_5$ mixing ratio (and $\tau$ $NO_3$ ) at 02:48, 03:20 and 04:06. These features correlate with small increases (less than 1 °C) in the temperature and indicate an influx of air from higher (warmer) layers within the nocturnal inversion, which were less impacted by ground level emissions of e.g. NO or other reactive trace gases. This is a strong indication of large gradients in $NO_3$ (and $N_2O_5$) at the site, which were corroborated by DOAS measurements of $NO_3$ at three different levels (Thieser et al., 2011).

In order to understand the factors which limit the $NO_3$ lifetimes during this night we first estimate the contribution of each constrained loss process for $NO_3$ and $N_2O_5$ to see if the summed loss (in the case of $N_2O_5$ scaled by $K_{eq}[NO_2]$, see Eq. 2) is





ACPD
11, 17825–17877, 2011



consistent with observations. Figure 5 reveals that the lifetime of $NO_3$ was dependent on $NO_2$ mixing ratios, with the largest lifetimes associated with low $NO_2$ mixing ratios. Such observations are frequently taken as evidence for an important contribution of $N_2O_5$ losses to $f_{ss}(NO_3)$ (see Eq. 2) and we consider these first.

## Loss of $N_2O_5$ to aerosols

The uptake coefficient for hydrolysis of $N_2O_5$ on aqueous, sulphate containing, tropospheric aerosol has been measured using laboratory surrogate aerosol (Mozurkewich and Calvert, 1988; Hu and Abbatt, 1997; Kane et al., 2001; Folkers et al., 2003; Badger et al., 2006; Griffiths and Cox, 2009) and a value of $\gamma \sim 0.04$ at high relative humidity has been recommended (IUPAC, 2010). This is consistent with the largest values of $\gamma$ derived from calculations using field observations of $NO_3$ and $N_2O_5$ (Allan et al., 1999; Aldener et al., 2006; Ambrose et al., 2007; Bertram et al., 2009; Brown et al., 2009). Both laboratory and field work indicate however that $N_2O_5$ uptake coefficients can be significantly lower in the presence of organic components or nitrate (see e.g. Mentel et al., 1999; Anttila et al., 2006; Bertram and Thornton, 2009; Griffiths et al., 2009; Riemer et al., 2009). Riemer et al. (2009) showed that the uptake coefficient of $N_2O_5$ on a pure inorganic aerosol depended on the sulphate to nitrate ratio with maximum values of $\gamma(N_2O_5) = 0.02$ on pure sulphate, which reduced to ~0.01 when the sulphate and nitrate masses were equivalent. Bertram et al (2009) measured $N_2O_5$ reactivity on ambient aerosol and found for one air sample a maximum value of $\gamma$ between 0.03 and 0.04 when the ratio of organic-to-sulphate particle mass was ~2.5. This decreased to 0.01 with an organic-to-sulphate ratio of 10. Bertram and Thornton (Bertram and Thornton, 2009) also describe the particle water molarity dependence of $\gamma(N_2O_5)$ on the uptake of $N_2O_5$ to $NH_3HSO_4$ aerosol. Maximum values of $\gamma$ $(N_2O_5) = 0.03$ were found when the $H_2O$ molarity was 20 or greater, but which decreased rapidly below this threshold. Given that the organic mass fraction of the particles was frequently above 50 % before 04:30, lower values of $\gamma$ than 0.03 will apply irrespective of the ni-





ACPD
11, 17825–17877, 2011



trate content. Not only the organic mass fraction of the aerosol but also the oxidation state of the condensed organic species influences the rates of uptake of both $N_2O_5$ and $NO_3$, either indirectly via the water fraction of the aerosol ($N_2O_5$) or directly via the number of double bonds available for $NO_3$ to react with.

During the night of 6–7 December the total aerosol surface area was low, consistent with relatively clean maritime air masses, with maximum values of about 90 $\mu m^2\ cm^{-3}$ at the beginning of the $NO_3/N_2O_5$ measurements and decreasing to ~30 $\mu m^2\ cm^{-3}$ at the end of the night. The organic-to-sulphate ratio was ~4 until 04:00 when it started decreasing to a value of ~0.3 to 0.4 clearly indicating a change in air mass to a more marine one at this time. The sulphate to (sulphate + nitrate) ratio was between ~0.6 and 0.9. The RH was above 90 % all the time so that, late in the night, with high sulphate content and high RH, aqueous aerosol should support a large uptake coefficient, i.e. up to a maximum value of ~0.04.

The total $NO_3$ loss rate, $f_{ss}(NO_3)$, calculated using an $N_2O_5$ uptake coefficient of 0.04 for the entire night is displayed in Fig. 6 (lower panel) where various contributors are compared. For most of the night, the low aerosol surface areas meant that $N_2O_5$ uptake to aerosol (RN2O5ASA) accounted for only a few percent to $f_{ss}(NO_3)$ with the exception of periods where the $NO_3$ lifetime was longest. For example, at 02:00 ~10 % of the calculated total loss was due to heterogeneous processing of $N_2O_5$. When we consider that, especially during the early stages of the measurement, the aerosol had a dominant organic component a lower value than 0.04 for $\gamma$ would be more realistic, which would further decrease the contribution of $N_2O_5$ loss. From 04:00 onwards, the contribution of $N_2O_5$ uptake to $f_{ss}(NO_3)$ diminished as the $NO_2$ mixing ratio decreased (shifting the $NO_3/N_2O_5$ equilibrium towards $NO_3$). At ~06:00 less than 5% of the measured loss frequency of $NO_3$ was due to $N_2O_5$ losses.





ACPD
11, 17825–17877, 2011



### Reaction of $N_2O_5$ with water vapour

Laboratory experiments (Wahner et al., 1998) have provided evidence for a slow reaction between $N_2O_5$ and $H_2O$, which, under certain circumstances, (e.g. low aerosol loading) can contribute to the loss of $N_2O_5$.

$$N_2O_5 + n\ H_2O \rightarrow 2\ HNO_3 + (n-1)\ H_2O \quad \text{(R3)}$$

The reaction was found to proceed with terms both linear and quadratic in $[H_2O]$ so that the loss rate coefficient ($k_{H_2O}$) is described by $k_{H_2O} = 2.5\times10^{-22}\ [H_2O] + 1.8\times10^{-39}\ [H_2O]^2\ s^{-1}$. Measurements of long $N_2O_5$ lifetimes at high relatively humidity (Brown et al., 2009) strongly suggest that the true value may be a factor 10 lower. We therefore assess the impact of this reaction on $NO_3$ lifetimes using $0.1\times k_{H_2O}$. This is displayed as Rwater in the lower panel of Fig. 6. At rates of $<1\times10^{-4}$, reaction with $H_2O$ has an insignificant impact on the overall loss rate of $N_2O_5$ (or $NO_3$) throughout the entire night.

### Dry deposition of $N_2O_5$

Assuming neutral stratification and zero surface resistance Geyer et al. (2001a) calculated an upper limit to the $N_2O_5$ loss frequency due to dry deposition within a 100 m deep nocturnal boundary layer as $0.3\times10^{-4}\ s^{-1}$. When multiplied by $k_2[NO_2]$, this results in a loss rate constant for $NO_3$ of $<1\times10^{-4}\ s^{-1}$, contributing insignificantly to the $NO_3$ lifetime (RddN2O5 in lower panel of Fig. 6).

### Gas-Phase reactions of $NO_3$

Known reaction partners for $NO_3$, which were constrained by measurements were NO, $\alpha$-pinene, isoprene and HCHO. The reactions of $NO_3$ with both NO and $\alpha$-pinene





ACPD
11, 17825–17877, 2011



have large rate coefficients ($k_4 = 2.6\times10^{-11}$, $k_5 = 6.2\times10^{-12}$ cm$^3$ molecule$^{-1}$ s$^{-1}$) whereas isoprene and HCHO react more slowly ($k_6 = 7\times10^{-13}$ cm$^3$ molecule$^{-1}$ s$^{-1}$, $k_7 = 5.6\times10^{-16}$ cm$^3$ molecule$^{-1}$ s$^{-1}$; Atkinson et al., 2004, 2006). At mixing ratios of less than 1 ppbv on this night HCHO did not contribute significantly to $NO_3$ removal and is not further considered. Likewise, isoprene mixing ratios on this night were less than those of $\alpha$-pinene and limonene and as isoprene reacts a factor ~10 slower than $\alpha$-pinene or limonene with $NO_3$, we do not need to consider Reaction (R6).

$$NO_3 + NO \rightarrow 2NO_2 \quad \text{(R4)}$$

$$NO_3 + \alpha - \text{pinene} \rightarrow \text{products} \quad \text{(R5)}$$

$$NO_3 + \text{isoprene} \rightarrow \text{products} \quad \text{(R6)}$$

$$NO_3 + \text{limonene} \rightarrow \text{products} \quad \text{(R7)}$$

$$NO_3 + HCHO \rightarrow HNO_3 + HCO \quad \text{(R8)}$$

The calculated, steady state, turnover loss rates of $NO_3$ for reaction with NO (RNO), $\alpha$-pinene (Rpinene) and limonene (Rlimo) are illustrated in Fig. 6 (lower panel). Loss of $NO_3$ due to reaction with $\alpha$-pinene and limonene was slow reflecting the low concentrations and emission rates of biogenic trace gases during late autumn at this site (Song et al., 2011), but still significant in the early part of the night, where its contribution easily exceeds that of heterogeneous losses. The reaction with NO is unimportant until ~04:00 but thereafter becomes the dominant $NO_3$ sink for the rest of the night and even at mixing ratios of just 5 pptv can account for the entire observed $NO_3$ loss until ~06:00. After 06:00, the reaction of NO accounts for ~30 % of the observed $NO_3$ loss rate. Note that fine structure on the $NO_3$ loss rate due to R4 (RNO) is due to noise as the measurements were made close to the NO detection limit.





ACPD
11, 17825–17877, 2011



## Loss of $NO_3$ to aerosols and via dry deposition

Laboratory experiments have characterised the efficiency of uptake of $NO_3$ to various environmental surfaces. Whereas the low solubility of $NO_3$ in water leads to low uptake coefficients ($\gamma_{NO_3} \leq 10^{-3}$) for interaction with aqueous droplets (Rudich et al., 1996), large values ($\gamma_{NO_3} \sim 0.1$) have been found for uptake to low volatility, unsaturated organic liquids (Moise et al., 2002; Gross and Bertram, 2009; Gross et al., 2009), such as those present in secondary organic aerosol. Uptake of $NO_3$ to urban aerosol (Tang et al., 2010) or organic aerosols (Gross et al., 2009) has been found to be orders of magnitude more efficient than $N_2O_5$ uptake to the same aerosol type. For the purpose of assessing the contribution of heterogeneous $NO_3$ loss to aerosol we have used a value of $\gamma = 0.1$, which most probably represents an upper limit to the true value. Despite the use of this large value, the loss of $NO_3$ to aerosol is not significant (RNO3ASA in the lower panel of Fig. 6) but nonetheless exceeds $N_2O_5$ loss rates via uptake to aerosol when $NO_2$ is low (i.e. when the $NO_3/N_2O_5$ equilibrium is not strongly partitioned towards $N_2O_5$) as seen between 02:00 and 04:00. As for $N_2O_5$, dry deposition (RddNO3) is insignificant if a loss rate of $0.3 \times 10^{-4}$ s$^{-1}$ is adopted (Geyer et al., 2001a).

## Summary

Some of the cleanest air-masses encountered at night in the campaign reached the measurement site in the night of 6–7 December and $NO_3$ lifetimes were correspondingly long. A large fraction (and sometimes all) of the $NO_3$ reactivity was accounted for with measured parameters as summarised in the lower panel of Fig. 6. The upper panel of Fig. 6 displays the measured $N_2O_5$ mixing ratios and those calculated from expression (5), which was obtained by reorganising expressions (1, 2 and 4):

$$[N_2O_5] = \frac{k_1 K_2 [NO_2]^2 [O_3]}{f_{ss}(NO_3)} \quad (5)$$





ACPD
11, 17825–17877, 2011



The predicted, steady-state mixing ratios of $N_2O_5$ are generally within a factor of 2–3 of those measured, though the strong, short-term variability in the measurements is not reproduced. This is presumably a result of low-time resolution measurement of some of the trace gases (e.g. terpenes) responsible for $NO_3$ loss.

Although the results suggest that the aerosol loss of $N_2O_5$ contributed up to 20 % to $NO_3$ losses early in the night, recall that the $\gamma$ used was most likely too high for aerosol with a dominant organic fraction and thus may be considered an upper limit. Missing reactivity (i.e. measured $NO_3$ lifetimes were shorter than calculated based on measured parameters) was apparent between circa 03:00 and 04:00 and also after 06:00. The deviation between measured and calculated $NO_3$ lifetimes is similar in direction and magnitude to that observed previously in marine air masses (Sommariva et al., 2007).

Considering that this air mass had spent several days over the ocean, it is conceivable that $CH_3SCH_3$ (not measured) could be an important contributor to $NO_3$ reactivity. Given a rate constant for reaction between $NO_3$ and $CH_3SCH_3$ of $1.1\times10^{-12}$ cm$^3$ molecule$^{-1}$ s$^{-1}$ (Atkinson et al., 2004) the missing reactivity observed at ~06:00 (about 0.005 s$^{-1}$) would be provided by ~200 pptv of $CH_3SCH_3$. Strong evidence for $CH_3SCH_3$ in this air mass could be found in AMS measurements of significant methane-sulphonic acid concentrations on the morning of 07.12.

As already mentioned, the plot of $NO_3$ lifetime versus $NO_2$ (Fig. 5) could be interpreted to indicate that indirect loss of $NO_3$ (i.e. via $N_2O_5$ removal) is an important contributor to $NO_3$ lifetimes. The discussion above indicates however, that the indirect losses are inefficient and a weak correlation between $NO_2$ and NO explains the dependence of $NO_3$ lifetimes on $NO_2$. At high $NO_2$ mixing ratios (e.g. 1–1.5 ppb) the calculated lifetimes are larger than measured. These data points were taken at the end of the night (after 06:00) and Fig. 6 also indicates missing reactivity during this period. In the absence of a significant change in wind direction, the plume like $NO_2$ increases (about 0.5 ppb) during this part of the night may indicate local ship emissions and an increase in reactivity towards $NO_3$ due to other trace gases co-emitted.





ACPD
11, 17825–17877, 2011



As a significant fraction of the $NO_3$ reactivity is accounted for by measured NO (which must have a local source) the use of a steady-state analysis for the later part of this night is not entirely appropriate. Local emissions of NO imply an increase in local $NO_2$ (at the expense of $O_3$). This does however not result in local $NO_3$ generation because the rate coefficient ($k_1$) is very low. This is compounded by the fact that $NO_3$ is lost via reaction with NO (also to make $NO_2$). The result is an apparently high production term (i.e. $NO_2$ and $O_3$ mixing ratios) combined with a low $NO_3$ concentration to derive an artificially low lifetime.

Low nighttime concentrations of NO have previously been reported to limit $NO_3$ lifetimes in a relatively clean coastal environment, which may be impacted by local NO emissions, e.g. from soil (Sommariva et al., 2007).

#### 4.1.2 23–24 November: mixed air from the continental and Huelva sectors

Measurements of $N_2O_5$ on this evening started at 20:00 UTC, about 2.5 h after sunset. The complete dataset, with meteorological information and other trace gas measurements is displayed in Fig. 7. Until midnight, the wind was mainly from the continental sector (close to 360 degrees) whereas after midnight it came mainly from the Huelva/Port sectors. Following a warm, cloud-free day, the night of 23–24 November was characterised by low wind speeds and a strong temperature inversion (temperature at 50 m was ~7 °C higher than at inlet height), implying a highly stratified nocturnal boundary layer. Back trajectories (Fig. 1) suggest that the air had travelled over the Atlantic before spending 1 day over central Spain- with the last 6–12 h within the BL.

$NO_2$ levels showed large variability during the night with mixing ratios between 1 and 13 ppbv, whereas NO was always close to zero (<2 pptv) until about 04:30 when a few pptv were observed. Some plume like $NO_2$ features were accompanied by plumes of similar duration in $SO_2$ (up to ~3 ppbv), HCHO (up to ~1.5 ppbv) and increases in the overall aerosol surface area, implying common, likely combustion related sources. This is especially apparent in the plumes at midnight and 05:00. For each of the $NO_2$ plumes at ~20:00, 21:30 and 23:00 there is a significant increase in the $N_2O_5$ mixing





ACPD
11, 17825–17877, 2011



ratio, caused by an increase in the $NO_3$ production rate. In contrast, $N_2O_5$ remains close to the detection limit for the entire $NO_2$ plume at midnight and reaches only low mixing ratios during the larger plumes at 05:00 and 06:30. Note that the $NO_2$ plume at ~23:00 (when $SO_2$ was close to zero) was accompanied by a positive gradient in the temperature, whereas the $NO_2/SO_2$ plume at midnight was accompanied by a negative temperature gradient. Similarly the $NO_2/SO_2$ plumes after 04:00 were accompanied by drops in temperature. The $NO_2/SO_2$ plumes were also accompanied by an increase in the aerosol surface area, caused by an increase in mainly the sulphate and nitrate content, but also the organic fraction of the aerosol. This is especially apparent at midnight.

Prior to midnight, $NO_2$ mixing ratios between ~1 and 6 ppbv and ozone levels of >25 ppbv resulted in large $NO_3$ production rates and the highest $N_2O_5$ concentrations in the entire campaign (~500 ppt) were measured. The high levels of $NO_2$ and moderately cold temperatures (283 K) meant that $N_2O_5$ was usually in greater than tenfold excess of the calculated $NO_3$ mixing ratio, and up to a factor of 50 greater at the peak of the $NO_2$ plumes. Prior to midnight, $\tau_{ss}(NO_3)$ was fairly constant at about 75–150 s but was essentially zero for the period between midnight and 01:00 during the $SO_2$ plume. Log-book entries report significant levels of malodorous gases at the site. The dependence of the $NO_3$ lifetime on $NO_2$ and $SO_2$ mixing ratios and aerosol surface area (ASA) is summarised in Fig. 8. The shortest $NO_3$ lifetimes are clearly associated with large $NO_2$ concentrations (upper panel), likewise $SO_2$ mixing ratios above 1 ppbv are always associated with very short $NO_3$ lifetimes and there is also weak anti-correlation with aerosol surface area. The observed $NO_2$ and aerosol surface area dependencies would appear to indicate that heterogeneous loss of $N_2O_5$ is important. Similar to the treatment above for the Atlantic sector we therefore assess (via Eq. 2) gas-phase and heterogeneous loss mechanisms for $NO_3$ and $N_2O_5$ which were constrained by measurements and also identify potential (unmeasured) reactive trace gases.





ACPD
11, 17825–17877, 2011



## Heterogeneous loss of $NO_3$ and $N_2O_5$

Compared to 7 December, the surface area available for interaction of aerosol with $N_2O_5$ or $NO_3$ was significantly larger on this night (factor of 2–3). The high levels of $NO_2$ observed result in large $N_2O_5/NO_3$ ratios, so that the heterogeneous losses would be expected to be more important for $N_2O_5$ than for $NO_3$. For this night the aerosol contained a very high organic component (up to 75 % of the aerosol mass) with organic/sulphate ratios as high as 15 early in the night and never decreasing below about 3. The sulphate/(sulphate + nitrate) ratio was also quite low (0.3–0.7).

As discussed above, $\gamma(N_2O_5)$ on such particles would be expected to be less than 0.04. For comparison, Zaveri et al. (Zaveri et al., 2010) have estimated an upper limit of $\gamma\ (N_2O_5) = 1\times10^{-3}$ for mixed sulphate/organic aerosol from a combustion source (power plant plume). The uptake coefficient for $NO_3$ is poorly defined but potentially a factor of 10 larger (Tang et al., 2010).

An absolute upper limit to the sum of direct and indirect $NO_3$ loss rates via heterogeneous uptake to aerosol was thus calculated using uptake coefficients of 0.04 for $N_2O_5$ and 0.5 for $NO_3$, the later representing diffusion limited uptake. This provides an estimate of the maximum contribution of heterogeneous reactions on aerosols to the $NO_3$ lifetime.

Figure 9 (lower panel) provides an overview of the relative importance of the constrained, direct and indirect loss processes for $NO_3$ on this night. Even though the uptake coefficients employed were upper limits, the calculated loss of $N_2O_5$ (RN2O5ASA) and $NO_3$ (RNO3ASA) to aerosols does not account entirely for the observed $NO_3$ loss frequency (black dots) before ~23:30 on 23 November. Despite the much larger uptake coefficient used for $NO_3$, its contribution to the total heterogeneous loss was similar to that of $N_2O_5$ as the $NO_3$–$N_2O_5$ partitioning was shifted towards $N_2O_5$ on this night with high $NO_2$ mixing ratios.

During the first $SO_2/NO_2$ plume (centred at midnight) the $NO_3$ lifetime was drastically shortened and heterogeneous processes contribute an upper limit of ~10 % to





ACPD
11, 17825–17877, 2011



the overall measured loss frequency of $NO_3$ (RN2O5ASA + RNO3ASA). Similarly, the summed effect of dry deposition of $NO_3$ and $N_2O_5$ (using the dry deposition rates listed above) can be disregarded as a major loss of either $NO_3$ or $N_2O_5$ (Rdd).

### Gas-Phase reactions of $NO_3$ and $N_2O_5$

Similar to 7 December, the homogeneous hydrolysis of $N_2O_5$ is not an important loss process in this air mass, contributing less than 1 % to the $NO_3$ reactivity (Rwater in the lower panel of Fig. 9). Close to zero levels of NO during most of this night also rule out a significant impact (RNO). The sum of the direct $NO_3$ loss rates due to BVOC (the sum of $\alpha$-pinene, limonene and isoprene, Rbiogen) contributes significantly to $NO_3$ loss before 23:00, but only a few percent during the $SO_2$ plumes. Further measured trace gases which can react with $NO_3$ are HCHO and aromatics. At a mixing ratio of close to 1 ppbv and a rate coefficient close to $5\times10^{-16}$ cm$^3$ molecule$^{-1}$ s$^{-1}$ (Atkinson et al., 2006) HCHO can contribute a negligible $1\times10^{-5}$ s$^{-1}$ to the overall $NO_3$ loss rate. Similarly, with respective room temperature rate coefficients of $<3\times10^{-17}$, $7\times10^{-17}$, $\sim4\times10^{-16}$ and $<6\times10^{-16}$ cm$^3$ molecule$^{-1}$ s$^{-1}$ (Atkinson and Arey, 2003), benzene (~80 pptv), toluene (~100 pptv), xylenes (sum of *p*, *m* and *o*-xylene was ~20 pptv) and ehylbenzene (8 pptv) all react too slowly with $NO_3$ to contribute significantly.

Under certain circumstances, $RO_2$ (formed e.g. from $NO_3$ initiated oxidation of $CH_3SCH_3$ or ozonolysis of BVOC) has been shown to contribute to $NO_3$ loss (Sommariva et al., 2009). On this night, $RO_2$ mixing ratios of up to 80 pptv were observed between ~midnight and 04:00 (Andrés-Heranández et al., to be submitted to the DOMINO special issue). In the absence of speciated $RO_2$ measurements we calculate the loss rate of $NO_3$ due to reaction with $RO_2$ assuming a rate coefficient of $2.3\times10^{-12}$ cm$^3$ molecule$^{-1}$ s$^{-1}$ taken from evaluated kinetic data (Atkinson et al., 2006). This results in $NO_3$ loss rates of $\sim5\times10^{-3}$ s$^{-1}$, which again is only a small fraction of the total loss rate (~4 % at midnight).





ACPD
11, 17825–17877, 2011



Clearly, the sum of constrained indirect and direct losses of $NO_3$ do not explain the short lifetimes observed during the $SO_2$ plumes. As heterogeneous processing cannot be enhanced in rate beyond that calculated using measured aerosol surface areas and upper limits for $\gamma(NO_3)$ and $\gamma(N_2O_5)$ we turn to potential gas-phase reactions, that were not constrained by measurements at the site.

### Unknown or undetermined reactions/loss processes

The aerosol surface area and trace gases which were measured provided only a fraction of the observed reactivity after midnight on 23–24 November. A clue to the missing reactivity may be provided by the very short $NO_3$ lifetimes (or absence of $N_2O_5$) when $SO_2$ was present at levels above ~1 ppbv (Figs. 7 and 8).

Whilst $SO_2$ itself does not react with $NO_3$, it may be co-emitted or co-located with emissions of more reactive traces gases. Two scenarios are considered below in which reduced sulphur species or unsaturated VOCs are responsible for efficient $NO_3$ loss during periods of enhanced $SO_2$ on this night.

A log-book entry describes strongly malodorous air at the measurement site on this (and several other) nights. Malodorous, reduced sulphur compounds (RSC) are often associated with oil refining, pulp/paper mill and waste treatment activities (Nunes et al., 2005; Pal et al., 2009; Toda et al., 2010) and we note that not only a huge oil-refinery complex but also Spain's largest pulp/paper mill is located in Huelva.

RSC with high reactivity to $NO_3$ are $CH_3SCH_3$ (DMS), $CH_3SSCH_3$ (DMDS) and $CH_3SH$. $NO_3$ lifetimes are known to be strongly influenced by DMS emissions in marine air masses (Allan et al., 2000; Aldener et al., 2006; Sommariva et al., 2009) but a large contribution to $NO_3$ loss in urban air has also been reported (Shon and Kim, 2006). The oxidation of RSC by $NO_3$ results in the formation of $SO_2$, HCHO and $RO_2$ (Jensen et al., 1992) with (modelled) $RO_2$ levels often exceeding those observed during daylight (Sommariva et al., 2009). The rate coefficients for reaction of DMS, DMDS and $CH_3SH$ with $NO_3$ are all close to $1\times10^{-12}$ cm$^3$ molecule$^{-1}$ s$^{-1}$, so that a to-





ACPD
11, 17825–17877, 2011



tal mixing ratio of these RSC of 4 ppbv would provide an equivalent reactivity of 0.1 $s^{-1}$. Whilst no measurements of RSC were available to support their potential role, we note that ppbv mixing ratios are not unrealistic as RSC emitted into a shallow, highly stratified boundary layer at night have no gas-phase loss mechanisms apart from reaction with $NO_3$. Human odour thresholds for $H_2S$, $CH_3SH$, $CH_3SCH_3$ and $CH_3SSCH_3$ are also in the ppbv regime (Kim et al., 2007; Pal et al., 2009). In order to capture the $NO_3$ lifetime dependence on $SO_2$, a reactive term, considering the presence of a trace gas at a constant fraction of the $SO_2$ mixing ratio and reacting with $NO_3$ with a rate constant of $1\times10^{-12}$ $cm^3$ $molecule^{-1}$ $s^{-1}$ (i.e. like RSC) was added to Eq. (2). The result is the grey area (RSO2) of Fig. 9 (lower panel). The RSC to $SO_2$ ratio was adjusted (to ~two) to approximately capture the large $NO_3$ loss rates at midnight, bringing the measured and modelled steady state lifetime in rough agreement. The measured and calculated $N_2O_5$ mixing ratios (expression 5) are plotted in the upper panel of Fig. 9. In the scenario which includes the reaction of $NO_3$ with RSC (blue lines) the $N_2O_5$ mixing ratios are well reproduced. Not including this reaction (red line) results in a large over prediction of $N_2O_5$ during the $NO_2$ plumes at ~midnight and 04:30, which coincide with peaks in $SO_2$ (see Fig. 7). Conversely, earlier during the night, the red lines better reproduce the observed $N_2O_5$ mixing ratios, which may be related to a small offset (~200 ppt) in the $SO_2$ measurement.

The co-incidental increases in nighttime aerosol surface area and the sulphate component of the aerosol is difficult to account for in the RSC scenario unless a sufficient rate of oxidation of $SO_2$ (i.e. by reaction with OH) is available. Nighttime OH could conceivably be generated by reactions of $RO_2$ with $NO_3$ (Platt et al., 1990; Geyer et al., 2003). The increase in particle sulphate at the maximum of the 3 ppbv $SO_2$ plume was ~0.5 $\mu g\, m^{-3}$, which would require oxidation via reaction with OH of 100 pptv of $SO_2$ and efficient transfer of the $H_2SO_4$ product to the particle phase. Assuming a total reaction time of 4 h (maximum transport time from Huelva), this would still require a constant nighttime OH concentration en route of $\sim2\times10^6$ molecule $cm^{-3}$, which appears unreasonably high.





ACPD
11, 17825–17877, 2011



Interactions between $NO_x$ and reduced sulphur thus provide an interesting but highly speculative explanation for some of the observations on this and other campaign nights, including short $NO_3$ lifetimes, high $RO_2$ levels and formation of HCHO and $SO_2$, though we note that plume like increases in $SO_2$ were not always accompanied by increases in HCHO as illustrated for this night in Fig. 7.

In a second scenario, we consider the coincident arrival of the $SO_2$, $NO_2$ and HCHO plumes to be due to their formation in a common combustion source, either related to shipping or oil-refinery activity. During this night the wind direction swept slowly from the continental sector to the Huelva sector with the plumes in $NO_2$ reflecting emissions from various point sources in the coastal-Huelva region. The short lifetimes of $NO_3$ after midnight reflect highly reactive air masses from Huelva, but not necessarily due to RSC. Hydrocarbon emissions related to the petrochemical industry, including unsaturated VOC such as 1,3-butadiene (Roberts et al., 2003) which are reactive towards $NO_3$ could then be responsible for the short $NO_3$ lifetimes. In this scenario, the source of the peroxy radicals observed on this night would be reaction of unsaturated hydrocarbons with either $NO_3$ or $O_3$. In this context note that $NO_3$ reacts at least a factor 10 more slowly with unsaturated, petrochemical-related hydrocarbons (e.g. the rate coefficient for $NO_3$ with 1,3-butadiene is $1.0\times10^{-13}$ cm$^3$ molecule$^{-1}$ s$^{-1}$) than with RSC so that mixing ratios of several tens of ppbv of the alkene would be necessary to explain the short $NO_3$ lifetimes. In summary, air from the Huelva sector and the port/coastal region close to Huelva was highly reactive towards $NO_3$ resulting in very short lifetimes which were controlled by gas-phase reactions and a diminished role for heterogeneous processes (either for $NO_3$ or $N_2O_5$). Whilst RSC and unsaturated VOC were proposed as potential reaction partners for $NO_3$ they were not constrained by measurements and for extended periods of the night (especially when $SO_2$ was observable) much of the reactivity is not accounted for.





ACPD
11, 17825–17877, 2011



### 4.1.3 26–27 November: air from the continental sector

On the night of 26–27 November, local wind directions indicated air masses originating from continental Spain which avoided large local cities and industrial centres such as Huelva or Sevilla. Back trajectories suggested that the air had spent the last two days over central Spain and northern France before reaching the site, gradually descending from ~3500m to ground level over this period with only the last 4–6 h spent at altitudes of less than 500 m. Local wind speeds during the night were between 2.5 and 5 $m\,s^{-1}$.

On this night, $NO_2$ levels were generally under 2 ppbv except for a plume-like increase to ~4 ppbv at ~20:00 on the evening of 26 November (Fig. 10). As was frequently observed for the continental sector, $NO_2$ was correlated with black carbon but not with $SO_2$, indicating that emission by road traffic was the most likely source. NO was close to the detection limit (2 ppt) during the whole night, except for some spikes due to very local (likely vehicular) emissions. The constancy of the NO mixing ratio through the night strongly suggests that the true value is zero and the 2 pptv is a residual from zero correction. $O_3$ levels were constant at ~25–30 ppbv. Levels of biogenic hydrocarbons (isoprene, pinene) were low (~10 ppt) as on other nights of the campaign. Mixing ratios of aromatics were similar to 23 Novermber (less than 100 pptv). Aerosol surface areas were between 25 and 80 $\mu m^2\,cm^{-3}$ and were correlated with $NO_2$. The aerosol was acidic ($NH_4^-/SO_4^{2-} = 0.6$) with a dominant organic fraction (the organic to sulphate ratio was ~4 until 04:00 when it slowly decreased to 2).

$N_2O_5$ could be measured above the detection limit at almost all times during this night, with maximum mixing ratios of ~100 pptv and steady-state $NO_3$-lifetimes up to 900 s. Intermediate to those observed for the Huelva and Atlantic sectors. The CRD and DOAS-derived $NO_3$ mixing ratios were in good agreement, especially after midnight. The observations are summarised in Fig. 10.

As in the discussion of the previous case studies, direct and indirect losses of $NO_3$ were assessed based on measured aerosol surface areas and trace gases. For this purpose, NO mixing ratios were assumed to be zero. The calculations are summarised





ACPD
11, 17825–17877, 2011



in Fig. 11. The upper panel displays calculated (Red line, Expression 5) and measured $N_2O_5$ mixing ratios. There is generally reasonable agreement (within a factor of ~2), although the calculated values do not capture the low mixing ratios between ~21:00 and 23:00. Turning to the lower panel, for the time period between midnight and 07:00, the presence of $\alpha$-pinene and limonene at mixing ratios of 5–10 pptv results in loss rates of $\sim 4 \times 10^{-3}\,s^{-1}$. The calculated $NO_3$ loss rate in this period thus exceeds that measured suggesting that reactivity is entirely accounted for by reasonably well constrained gas-phase reactions. This allows us to estimate upper bounds for the rates of all other loss mechanisms, including uptake to aerosol on this night. The rate of direct loss of $NO_3$ to the organic component of the aerosol is of major uncertainty as the nature of the organic fraction (and thus availability of e.g. double bonds with which $NO_3$ can react) is unknown. A value of $\gamma$ $NO_3 = 0.1$ contributes only insignificantly to the $NO_3$ lifetime whereas a value of 0.5 (diffusion limited uptake) would increase the discrepancy between observed and calculated lifetimes. A similar effect would be obtained by use of a large value (e.g. 0.1) for $\gamma$ ($N_2O_5$). On this night, the organic to sulphate ratio was ~2–4 and the sulphate to (sulphate + nitrate) ratio was fairly constant at 0.6, implying a more likely value of $\gamma$ ($N_2O_5$) of ~0.01 (Riemer et al., 2009), which is also consistent with our observations.

In the first half of the night (up to ~midnight) $NO_3$ lifetimes were much shorter and highly variable, with loss rates up to $0.05\,s^{-1}$ (lifetimes of just 200s). We can rule out that this increase in the $NO_3$ loss frequency is due to a change in reactivity of the aerosol to either $N_2O_5$ or $NO_3$. Neither the aerosol composition (i.e., organic, nitrate and sulphate fractions and acidity) nor the relative humidity changed significantly during the night so a large change in $\gamma$ (factor 10) is not anticipated. Also, the large variability in the loss frequency is not mirrored by changes in aerosol surface area, but is most likely associated with fluctuations in rates of vertical mixing within a highly stratified nocturnal boundary layer, with longer lived $NO_3$ present in higher layers. Inspection of the temperature and $N_2O_5$ trends during this night reveals significant correlation, with higher temperatures (i.e. air from higher altitudes) bringing more $NO_3$. Measurements





ACPD
11, 17825–17877, 2011



of a strong vertical gradient in $N_2O_5$ on this night (Thieser et al., 2011) confirm this interpretation.

## 5 Summary and conclusions

Measurements of $N_2O_5$ and steady-state calculations of $NO_3$ lifetimes during the DOMINO campaign revealed stark differences according to the type of air mass encountered. The longest lifetimes (~30 min) of $NO_3$ were encountered in air masses arriving from the Atlantic sector. Air from the Huelva urban (petrochemical and industrial) sector had high production rates of $NO_3$, but frequently concentrations close to the detection limit and lifetimes of only a few seconds. The high reactivity could only be partially accounted for by measured trace gases and aerosol surface areas. Lifetimes of $NO_3$ were always very short when $SO_2$ was observed at the site, either due to reactions of $NO_3$ with RSC or due to common or co-located emissions (e.g. combustion) sources of other reactive trace gases. The relationship between the $NO_3$ lifetime, $SO_2$, $NO_2$ and ASA over the course of the entire campaign is illustrated in Fig. 12. Clearly, polluted air masses ($NO_2$ or $SO_2$>2 ppbv) do not support long $NO_3$ lifetimes.

$NO_3$ in air from the continental sector had lifetimes which were similar to other forested areas (e.g. (Crowley et al., 2010)), but which were occasionally significantly shortened, presumably due to the impact of emissions from industrial activity. In general these results show that $NO_3$ (or $N_2O_5$) mixing ratios in air masses from urban and industrial centres were controlled by gas-phase reactions of $NO_3$ and cannot be accurately estimated from production terms (e.g. $NO_2$ and $O_3$ mixing ratios) and measured BVOC and aerosol. However, the combination of high $NO_3$ production rates and short lifetimes frequently observed during the campaign implies large nocturnal processing rates for the VOCs mainly responsible for $NO_3$ loss, and thus a high production rate of organic peroxy radicals and secondary oxidation products, such as carbonyl compounds and organic nitrates/ nitric acid.





ACPD
11, 17825–17877, 2011



A large variability in the boundary layer $NO_3$ loss frequency was observed, which was related to vertical transport, longer lifetimes being associated with air masses from higher altitudes as previously observed (see e.g. Allan et al., 2002; Geyer and Stutz, 2004; Brown et al., 2007). Whilst the ground based measurements presented here can provide only tentative evidence for this, DOAS measurements of $NO_3$ during the campaign reveal strong altitude gradients, sometimes as much as a factor of ~10 change in $NO_3$ mixing ratios within the boundary layer (Thieser et al., 2011).

In many remote air masses, the efficiency of nocturnal loss of $NO_x$ to particulate phase or to long-lived reservoir species (e.g. $HNO_3$) which may undergo deposition, will depend both on the absolute and relative rates of processing of $NO_3$ (in gas-phase reactions) and $N_2O_5$ (in heterogeneous reactions). If direct loss processes of $NO_3$ are slow and $N_2O_5$ uptake to particles is efficient, the $NO_3$-$N_2O_5$ equilibrium-pair represents only a temporary $NO_x$ reservoir. $N_2O_5$ or $NO_3$ formed in the night will release $NO_x$ at sunrise as $NO_3$ lifetimes are shortened by photolysis (to form both NO and $NO_2$) and reaction with NO (to form $NO_2$). $N_2O_5$ decomposes thermally to $NO_2$ and $NO_3$, so that $NO_x$ is recovered and available for $O_3$ production. In the present campaign, nighttime lifetimes of $NO_3$ were generally so short that efficient irreversible loss of $NO_x$ occurred. $NO_3$ lifetimes of just a few minutes imply that the rate of loss of boundary layer $NO_x$ is approximately equal to the rate of $NO_3$ formation i.e.

$$L_{NO_x} \approx n \cdot k_1 [NO_2][O_3] \quad (6)$$

where the factor $n$ is 1 if $NO_3$ is lost only directly (e.g. by reaction with VOC) and is 2 if $NO_3$ is lost indirectly only via $N_2O_5$ formation and reaction as two $NO_2$ are required to make each $N_2O_5$ molecule. For the present campaign we have shown that, when produced at high rates, $NO_3$ is lost predominantly by direct routes, so that $n$ should be close to 1. Figure 13 displays the integrated $NO_x$ losses via reaction of $NO_2$ with $O_3$ for the three case studies outlined above. Over the course of a 12 h night between 0.8 and 1.8 ppbv of $NO_x$ were removed from the boundary layer, resulting in average loss rates of 1.9–4.2×$10^{-5}$ ppbv of $NO_2$ per second. Assuming that $NO_3$ is lost entirely by





ACPD
11, 17825–17877, 2011



reaction with VOC (and not by $NO_3$ or $N_2O_5$ uptake to aerosol), this is also the loss rate of VOC over the same period. For comparison, a 12 h, daytime loss of $NO_2$ via reaction with OH of $2\times10^{-5}\,s^{-1}$ would be obtained for average OH and $NO_2$ mixing ratios of 0.04 and 2000 ppt, respectively, though the greater daytime boundary layer depth would favour the OH mechanism.

*Acknowledgements.* We are indebted to the National Institute for Aerospace Technology (INTA) for hosting the campaign and to Monica Martinez (Max-Planck-Institut) for campaign organisation and management. We thank Pablo Hidalgo for information related to industrial activity in the Huelva area.

The service charges for this open access publication have been covered by the Max Planck Society.

## References

Aldener, M., Brown, S. S., Stark, H., Williams, E. J., Lerner, B. M., Kuster, W. C., Goldan, P. D., Quinn, P. K., Bates, T. S., Fehsenfeld, F. C., and Ravishankara, A. R.: Reactivity and loss mechanisms of $NO_3$ and $N_2O_5$ in a polluted marine environment: Results from in situ measurements during New England Air Quality Study 2002, J. Geophys. Res.-Atmos., 111, D23S73, doi:10.1029/2006JD007252, 2006.

Allan, B. J., Carslaw, N., Coe, H., Burgess, R. A., and Plane, J. M. C.: Observations of the nitrate radical in the marine boundary layer, J. Atmos. Chem., 33, 129–154, 1999.

Allan, B. J., McFiggans, G., Plane, J. M. C., Coe, H., and McFadyen, G. G.: The nitrate radical in the remote marine boundary layer, J. Geophys. Res.-Atmos., 105, 24191–24204, 2000.

Allan, B. J., Plane, J. M. C., Coe, H., and Shillito, J.: Observations of $NO_3$ concentration profiles in the troposphere, J. Geophys. Res.-Atmos., 107, 4588, doi:10.1029/2002jd002112, 2002.

Ambrose, J. L., Mao, H., Mayne, H. R., Stutz, J., Talbot, R., and Sive, B. C.: Nighttime nitrate radical chemistry at Appledore island, Maine during the 2004 international consortium for atmospheric research on transport and transformation, J. Geophys. Res.-Atmos., 112, D21302, doi:101.1029/2007JD008756, 2007.

Anttila, T., Kiendler-Scharr, A., Tillmann, R., and Mentel, T. F.: On the reactive uptake of gaseous compounds by organic-coated aqueous aerosols: Theoretical analysis and ap-





ACPD

11, 17825–17877, 2011



plication to the heterogeneous hydrolysis of $N_2O_5$, J. Phys. Chem. A, 110, 10435–10443, 2006.
Atkinson, R. and Arey, J.: Atmospheric degradation of volatile organic compounds, Chem. Rev., 103, 4605–4638, 2003.
Atkinson, R., Baulch, D. L., Cox, R. A., Crowley, J. N., Hampson, R. F., Hynes, R. G., Jenkin, M. E., Rossi, M. J., and Troe, J.: Evaluated kinetic and photochemical data for atmospheric chemistry: Volume I – gas phase reactions of $O_x$, $HO_x$, $NO_x$ and $SO_x$ species, Atmos. Chem. Phys., 4, 1461–1738, doi:10.5194/acp-4-1461-2004, 2004.
Atkinson, R., Baulch, D. L., Cox, R. A., Crowley, J. N., Hampson, R. F., Hynes, R.G., Jenkin, M. E., Rossi, M. J., and Troe, J.: Evaluated kinetic and photochemical data for atmospheric chemistry: Volume II – reactions of organic species, Atmos. Chem. Phys., 3625–4055, doi:10.5194/acp-6-3625-2006, 2006.
Badger, C. L., Griffiths, P. T., George, I., Abbatt, J. P. D., and Cox, R. A.: Reactive uptake of $N_2O_5$ by aerosol particles containing mixtures of humic acid and ammonium sulfate, J. Phys. Chem. A, 110, 6986–6994, 2006.
Bertram, T. H. and Thornton, J. A.: Toward a general parameterization of $N_2O_5$ reactivity on aqueous particles: the competing effects of particle liquid water, nitrate and chloride, Atmos. Chem. Phys., 9, 8351–8363, doi:10.5194/acp-9-8351-2009, 2009.
Bertram, T. H., Thornton, J. A., Riedel, T. P., Middlebrook, A. M., Bahreini, R., Bates, T. S., Quinn, P. K., and Coffman, D. J.: Direct observations of $N_2O_5$ reactivity on ambient aerosol particles, Geophys. Res. Lett., 36, L19803, doi:10.1029/2009GL040248, 2009.
Brown, S. S., Dube, W. P., Fuchs, H., Ryerson, T. B., Wollny, A. G., Brock, C. A., Bahreini, R., Middlebrook, A. M., Neuman, J. A., Atlas, E., Roberts, J. M., Osthoff, H. D., Trainer, M., Fehsenfeld, F. C., and Ravishankara, A. R.: Reactive uptake coefficients for $N_2O_5$ determined from aircraft measurements during the Second Texas Air Quality Study: Comparison to current model parameterizations, J. Geophys. Res.-Atmos., 114, D00F10, doi:10.1029/2008JD011679, 2009.
Brown, S. S., Dube, W. P., Osthoff, H. D., Wolfe, D. E., Angevine, W. M., and Ravishankara, A. R.: High resolution vertical distributions of $NO_3$ and $N_2O_5$ through the nocturnal boundary layer, Atmos. Chem. Phys., 7, 139–149, doi:10.5194/acp-7-139-2007, 2007.
Brown, S. S., Ryerson, T. B., Wollny, A. G., Brock, C. A., Peltier, R., Sullivan, A. P., Weber, R. J., Dube, W. P., Trainer, M., Meagher, J. F., Fehsenfeld, F. C., and Ravishankara, A. R.: Variability in nocturnal nitrogen oxide processing and its role in regional air quality, Science,





ACPD
11, 17825–17877, 2011



311, 67–70, 2006.
Brown, S. S., Stark, H., and Ravishankara, A. R.: Applicability of the steady state approximation to the interpretation of atmospheric observations of $NO_3$ and $N_2O_5$, J. Geophys. Res.-Atmos., 108, 4539, doi:10.1029/2003JD003407, 2003a.
Brown, S. S., Stark, H., Ryerson, T. B., Williams, E. J., Nicks, D. K., Trainer, M., Fehsenfeld, F. C., and Ravishankara, A. R.: Nitrogen oxides in the nocturnal boundary layer: Simultaneous in situ measurements of $NO_3$, $N_2O_5$, $NO_2$, NO, and $O_3$, J. Geophys. Res.-Atmos., 108, 4299, doi:10.1029/2002JD002917, 2003b.
Carslaw, N., Carpenter, L. J., Plane, J .M. C., Allan, B. J., Burgess, R. A., Clemitshaw, K. C., Coe, H., and Penkett, S.A.: Simultaneous observations of nitrate and peroxy radicals in the marine boundary layer, J. Geophys. Res.-Atmos., 102, 18917–18933, 1997a.
Carslaw, N., Plane, J. M. C., Coe, H., and Cuevas, E.: Observations of the nitrate radical in the free troposphere at Izana de Tenerife, J. Geophys. Res.-Atmos., 102, 10613–10622, 1997b.
Crowley, J. N., Schuster, G., Pouvesle, N., Parchatka, U., Fischer, H., Bonn, B., Bingemer, H., and Lelieveld, J.: Nocturnal nitrogen oxides at a rural mountain site in south-western Germany, Atmos. Chem. Phys., 10, 2795–2812, doi:10.5194/acp-10-2795-2010, 2010.
Diesch, J.-M., Drewnick, F., von der Weiden-Reinmüller, S. L., Martinez-Harder, M., and Borrmann, S.: Variability of Aerosol, Trace Gas and Meteorological Characteristics associated with Continental, Urban and Marin Air Masses in the Southwestern Mediterranean, Atmos. Chem. Phys. Discuss., to be submitted, 2011.
Draxler, R. R. and Rolph, G. D.: HYSPLIT (HYbrid Single-Particle Lagrangian Integrated Trajectory), Model access via NOAA ARL READY Website at: http://ready.arl.noaa.gov/HYSPLIT.php. NOAA Air Resources Laboratory, Silver Spring, MD, USA, 2011.
Folkers, M., Mentel, T. F., and Wahner, A.: Influence of an organic coating on the reactivity of aqueous aerosols probed by the heterogeneous hydrolysis of $N_2O_5$, Geophys. Res. Lett., 30, 1644, doi:10.1029/2003GL017168, 2003.
Geyer, A. and Stutz, J.: Vertical profiles of $NO_3$, $N_2O_5$, $O_3$, and $NO_x$ in the nocturnal boundary layer: 2. Model studies on the altitude dependence of composition and chemistry (vol 109, art no D16399, 2004), J. Geophys. Res.-Atmos., 109, doi:10.1029/2004JD0052172004, 2004.
Geyer, A., Ackermann, R., Dubois, R., Lohrmann, B., Muller, T., and Platt, U.: Long-term observation of nitrate radicals in the continental boundary layer near Berlin, Atmos. Environ., 35, 3619–3631, 2001a.
Geyer, A., Alicke, B., Konrad, S., Schmitz, T., Stutz, J., and Platt, U.: Chemistry and oxidation





ACPD
11, 17825–17877, 2011



capacity of the nitrate radical in the continental boundary layer near Berlin, J. Geophys. Res.-Atmos., 106, 8013–8025, 2001b.
Geyer, A., Bachmann, K., Hofzumahaus, A., Holland, F., Konrad, S., Klupfel, T., Patz, H. W., Perner, D., Mihelcic, D., Schafer, H. J., Volz-Thomas, A., and Platt, U.: Nighttime formation of peroxy and hydroxyl radicals during the BERLIOZ campaign: Observations and modeling studies, J. Geophys. Res.-Atmos., 108, 8249, doi:10.1029/2001JD000656, 2003.
Gordon, I. E., Rothman, L. S., Gamache, R. R., Jacquemart, D., Boone, C., Bernath, P. F., Shephard, M. W., Delamere, J. S., and Clough, S. A.: Current updates of the water-vapor line list in HITRAN: A new "diet" for air-broadened half-widths, J. Quant. Spectrosc. Radiat. Transfer, 108, 389–402, 2007.
Griffiths, P. T. and Cox, R. A.: Temperature dependence of heterogeneous uptake of $N_2O_5$ by ammonium sulfate aerosol, Atmos. Sci. Lett., 10, 159–163, 2009.
Griffiths, P. T., Badger, C. L., Cox, R. A., Folkers, M., Henk, H. H., and Mentel, T. F.: Reactive uptake of $N_2O_5$ by aerosols containing dicarboxylic acids. Effect of particle phase, composition, and nitrate content, J. Phys. Chem. A, 113, 5082–5090, 2009.
Gross, S. and Bertram, A. K.: Products and kinetics of the reactions of an alkane monolayer and a terminal alkene monolayer with $NO_3$ radicals, J. Geophys. Res.-Atmos., 114, D02307, doi:10.1029/2008JD010987, 2009.
Gross, S., Iannone, R., Xiao, S., and Bertram, A. K.: Reactive uptake studies of $NO_3$ and $N_2O_5$ on alkenoic acid, alkanoate, and polyalcohol substrates to probe nighttime aerosol chemistry, Phys. Chem. Chem. Phys., 11, 7792–7803, 2009.
Heintz, F., Platt, U., Flentje, H., and Dubois, R.: Long-term observation of nitrate radicals at the tor station, Kap Arkona (Rugen), J. Geophys. Res.-Atmos., 101, 22891–22910, 1996.
Hu, J. H. and Abbatt, J. P. D.: Reaction probabilities for $N_2O_5$ hydrolysis on sulfuric acid and ammonium sulfate aerosols at room temperature, jpc-A, 101, 871–878, 1997.
IUPAC. Subcommittee for gas kinetic data evaluation, in: Evaluated kinetic data, edited by: Ammann, M., Atkinson, R., Cox, R. A., Crowley, J. N., Hynes, R. G., Jenkin, M. E., Mellouki, W., Rossi, M. J., Troe, J. and Wallington, T. J., http://www.iupac-kinetic.ch.cam.ac.uk/, 2010.
Jensen, N. R., Hjorth, J., Lohse, C., Skov, H., and Restelli, G.: Products and mechanisms of the gas-phase reactions of $NO_3$ with $CH_3SCH_3$, $CD_3SCD_3$, $CH_3SH$ and $CH_3SSCH_3$, J. Atmos. Chem., 14, 95–108, 1992.
Kane, S. M., Caloz, F., and Leu, M. T.: Heterogeneous uptake of gaseous $N_2O_5$ by $(NH_4)_2SO4$, $NH_4HSO_4$, and $H_2SO_4$ aerosols, J. Phys. Chem. A, 105, 6465–6470, 2001.





ACPD
11, 17825–17877, 2011



Kelly, T. J., and Fortune, C. R.: Continuous monitoring of gaseous formaldehyde using an improved fluorescence approach, Int. J. Environ. Anal. Chem, 54, 249–263, 1994.
Kim, K. H., Jeon, E. C., Choi, Y. J., and Koo, Y. S.: The emission characteristics and the related malodour intensities of gaseous reduced sulfur compounds (RSC) in a large industrial complex (40, p. 4478, 2006), Atmos. Environ., 41, p. 3728, 2007.
Kley, D. and McFarland, M.: Chemiluminescence detector for NO and $NO_2$, Atmos. Technol., 12, 63–69, 1980.
Martinez, M., Perner, D., Hackenthal, E. M., Kulzer, S., and Schutz, L.: $NO_3$ at Helgoland during the NORDEX campaign in October 1996, J. Geophys. Res., 105, 22685–22695, 2000.
Mentel, T. F., Sohn, M., and Wahner, A.: Nitrate effect in the heterogeneous hydrolysis of dinitrogen pentoxide on aqueous aerosols, Phys. Chem. Chem. Phys., 1, 5451–5457, 1999.
Merten, A., Tschritter, J., and Platt, U.: Design of differential optical absorption spectroscopy long-path telescopes based on fiber optics, Appl. Opt., 50, 738–754, 2011.
Moise, T., Talukdar, R. K., Frost, G. J., Fox, R. W., and Rudich, Y.: Reactive uptake of $NO_3$ by liquid and frozen organics, J. Geophys. Res.-Atmos., 107(D2), 4014, doi:10.1029/2001JD000334, 2002.
Mozurkewich, M. and Calvert, J. G.: Reaction probability of $N_2O_5$ on aqueous aerosols, J. Geophys. Res.-Atmos., 93, 15889–15896, 1988.
Nunes, L. S. S., Tavares, T. M., Dippel, J., and Jaeschke, W.: Measurements of atmospheric concentrations of reduced sulphur compounds in the All Saints Bay area in Bahia, Brazil, J. Atmos. Chem., 50, 79–100, 2005.
Osthoff, H. D., Pilling, M. J., Ravishankara, A. R., and Brown, S. S.: Temperature dependence of the $NO_3$ absorption cross-section above 298 K and determination of the equilibrium constant for $NO_3 + NO_2 <-> N_2O_5$ at atmospherically relevant conditions, Phys. Chem. Chem. Phys., 9, 5785–5793, 2007.
Pal, R., Kim, K. H., Jeon, E. C., Song, S. K., Shon, Z. H., Park, S. Y., Lee, K. H., Hwang, S. J., Oh, J.M., and Koo, Y. S.: Reduced sulfur compounds in ambient air surrounding an industrial region in Korea, Environ. Monit. Assess., 148, 109–125, 2009.
Platt, U., Lebras, G., Poulet, G., Burrows, J. P., and Moortgat, G.: Peroxy-radicals from night-time reactions of $NO_3$ with organic compounds, Nature, 348, 147–149, 1990.
Pöhler, D., Vogel, L., Friess, U., and Platt, U.: Observation of halogen species in the Amundsen Gulf, Arctic, by active long-path differential optical absorption spectroscopy, Proc. Natl. Acad. Sci. USA, 107, 6582–6587, 2010.





ACPD
11, 17825–17877, 2011



Riemer, N., Vogel, H., Vogel, B., Anttila, T., Kiendler-Scharr, A., and Mentel, T. F.: Relative importance of organic coatings for the heterogeneous hydrolysis of $N_2O_5$ during summer in Europe, J. Geophys. Res.-Atmos., 114, D17307 doi: 10.1029/2008JD011369, 2009.

Roberts, J. M., Jobson, B. T., Kuster, W., Goldan, P., Murphy, P., Williams, E., Frost, G., Riemer, D., Apel, E., Stroud, C., Wiedinmyer, C., and Fehsenfeld, F.: An examination of the chemistry of peroxycarboxylic nitric anhydrides and related volatile organic compounds during Texas Air Quality Study 2000 using ground-based measurements, J. Geophys. Res.-Atmos., 108, 4495, doi:10.1029/2003jd003383, 2003.

Rudich, Y., Talukdar, R. K., Ravishankara, A. R., and Fox, R. W.: Reactive uptake of $NO_3$ on pure water and ionic solutions, J. Geophys. Res., 101, 21023–21031, 1996.

Schuster, G., Labazan, I., and Crowley, J. N.: A cavity ring down/cavity enhanced absorption device for measurement of ambient NO3 and $N_2O_5$, Atmos. Meas. Tech., 2, 1–13, doi:10.5194/amt-2-1-2009, 2009.

Shon, Z. H. and Kim, K. H.: Photochemical oxidation of reduced sulfur compounds in an urban location based on short time monitoring data, Chemosphere, 63, 1859–1869, 2006.

Sommariva, R., Osthoff, H. D., Brown, S. S., Bates, T. S., Baynard, T., Coffman, D., de Gouw, J. A., Goldan, P. D., Kuster, W. C., Lerner, B. M., Stark, H., Warneke, C., Williams, E. J., Fehsenfeld, F. C., Ravishankara, A. R., and Trainer, M.: Radicals in the marine boundary layer during NEAQS 2004: a model study of day-time and night-time sources and sinks, Atmos. Chem. Phys., 9, 3075–3093, doi:10.5194/acp-9-3075-2009, 2009.

Sommariva, R., Pilling, M. J., Bloss, W. J., Heard, D. E., Lee, J. D., Fleming, Z. L., Monks, P. S., Plane, J. M. C., Saiz-Lopez, A., Ball, S. M., Bitter, M., Jones, R. L., Brough, N., Penkett, S. A., Hopkins, J. R., Lewis, A. C., and Read, K. A.: Night-time radical chemistry during the NAMBLEX campaign, Atmos. Chem. Phys., 7, 587–598, doi:10.5194/acp-7-587-2007, 2007.

Song, W., Williams, J., Yassaa, N., Regelin, E., Harder, H., Martinez, M., Carnero, J. A. A., Hidalgo, P. J., Bozem, H., and Lelieveld, J.: Characterization of biogenic enantiomeric monoterpenes and anthropogenic BTEX Compounds at a Mediterranean Stone pine Forest site in Southern Spain, to be submitted, Atmos. Chem. Phys. Discuss., 2011.

Stutz, J. and Platt, U.: Numerical analysis and estimation of the statistical error of differential optical absorption spectroscopy measurements with least-squares methods, Appl. Opt., 35, 6041–6053, 1996.

Tang, M. J., Thieser, J., Schuster, G., and Crowley, J. N.: Uptake of $NO_3$ and $N_2O_5$ to Saharan





ACPD
11, 17825–17877, 2011



dust, ambient urban aerosol and soot: a relative rate study, Atmos. Chem. Phys., 10, 2965–2974, doi:10.5194/acp-10-2965-2010, 2010.
Thieser et al.: Manuscript in preparation for submision, DOMINO special issue, Atmos. Chem. Phys. Discuss., 2011.
Toda, K., Obata, T., Obolkin, V. A., Potemkin, V. L., Hirota, K., Takeuchi, M., Arita, S., Khodzher, T. V., and Grachev, M. A.: Atmospheric methanethiol emitted from a pulp and paper plant on the shore of Lake Baikal, Atmos. Environ., 44, 2427–2433, 2010.
Vandaele, A. C., Hermans, C., Simon, P. C., Carleer, M., Colin, R., Fally, S., Merienne, M. F., Jenouvrier, A., and Coquart, B.: Measurements of the $NO_2$ absorption cross-section from 42 000 $cm^{-1}$ to 10 000 $cm^{-1}$ (238–1000 nm) at 220 K and 294 K, J. Quant. Spectrosc. Radiat. Transfer, 59, 171–184, 1998.
Voigt, S., Orphal, J., Bogumil, K., and Burrows, J. P.: The temperature dependence (203–293 K) of the absorption cross sections of $O_3$ in the 230-850 nm region measured by Fourier-transform spectroscopy, J. Photochem. Photobiol. A-Chem., 143, 1–9, 2001.
Wagner, C., Hanisch, F., de Coninck, H. C., Holmes, N. S., Schuster, G., and Crowley, J. N.: The interaction of $N_2O_5$ with mineral dust: Aerosol flow tube and Knudsen reactor studies, Atmos. Chem. Phys., 8, 91–109, doi:10.5194/acp-8-91-2008, 2008.
Wahner, A., Mentel, T. F., and Sohn, M.: Gas-phase reaction of $N_2O_5$ with water vapor: Importance of heterogeneous hydrolysis of $N_2O_5$ and surface desorption of $HNO_3$ in a large teflon chamber, Geophys. Res. Lett., 25, 2169–2172, 1998.
Wayne, R. P., Barnes, I., Biggs, P., Burrows, J. P., Canosa-Mas, C. E., Hjorth, J., Le Bras, G., Moortgat, G. K., Perner, D., Poulet, G., Restelli, G., and Sidebottom, H.: The nitrate radical: Physics, chemistry, and the atmosphere, AE, 25A, 1–206, 1991.
Yokelson, R. J., Burkholder, J. B., Fox, R. W., Talukdar, R. K., and Ravishankara, A. R.: Temperature-dependence of the $NO_3$ absorption spectrum, J. Phys. Chem., 98, 13144–13150, 1994.
Zaveri, R. A., Berkowitz, C. M., Brechtel, F. J., Gilles, M. K., Hubbe, J. M., Jayne, J. T., Kleinman, L. I., Laskin, A., Madronich, S., Onasch, T. B., Pekour, M. S., Springston, S. R., Thornton, J. A., Tivanski, A. V., and Worsnop, D. R.: Nighttime chemical evolution of aerosol and trace gases in a power plant plume: Implications for secondary organic nitrate and organosulfate aerosol formation, $NO_3$ radical chemistry, and $N_2O_5$ heterogeneous hydrolysis, J. Geophys. Res.-Atmos., 115, D12304, doi:10.1029/2009jd013250, 2010.





ACPD
11, 17825–17877, 2011



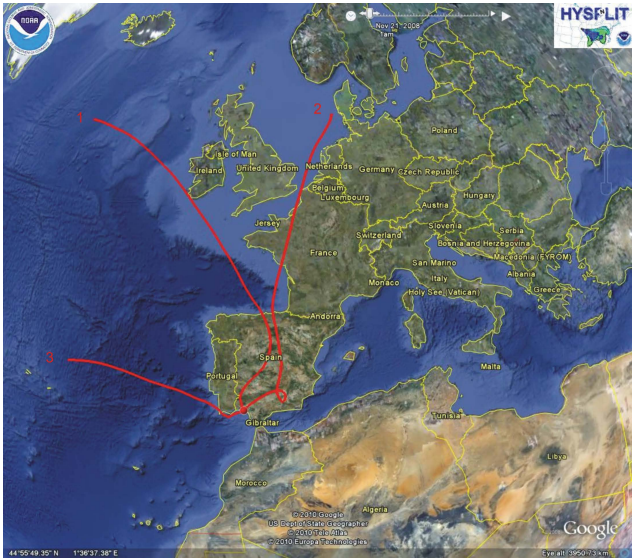


**Fig. 1.** Location of the measurement site with three 72-h HYSPLIT back-trajectories of air masses reaching the site at midnight on 24 November 2008 (1, Huelva sector), 27 November 2008 (2, continental sector) and 7 December 2008 (3, Atlantic sector).





ACPD
11, 17825–17877, 2011



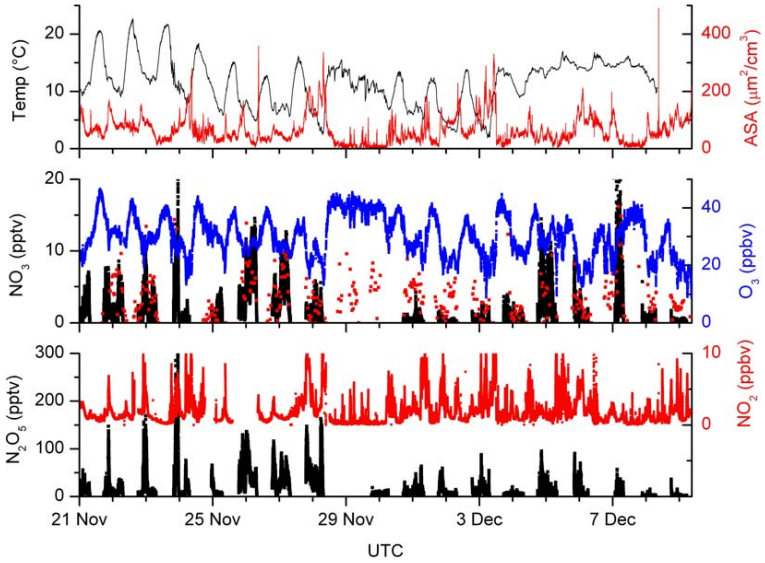


**Fig. 2.** Campaign overview of measured $N_2O_5$, $NO_2$ and $O_3$ mixing ratios, aerosol surface area (ASA), temperature and calculated CRD-$NO_3$ mixing ratios. The red $NO_3$ datapoints are LP-DOAS measurements. x-axis ticks are at midnight.





ACPD
11, 17825–17877, 2011



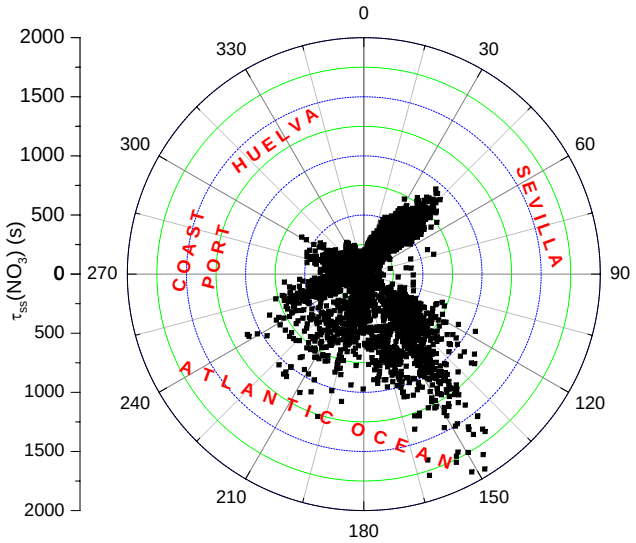


**Fig. 3.** Wind-direction dependence of $NO_3$ lifetimes. Although ~50 % of the airmasses encountered at night came from the Huelva sector, $NO_3$ lifetimes in this sector were always very short.





ACPD
11, 17825–17877, 2011



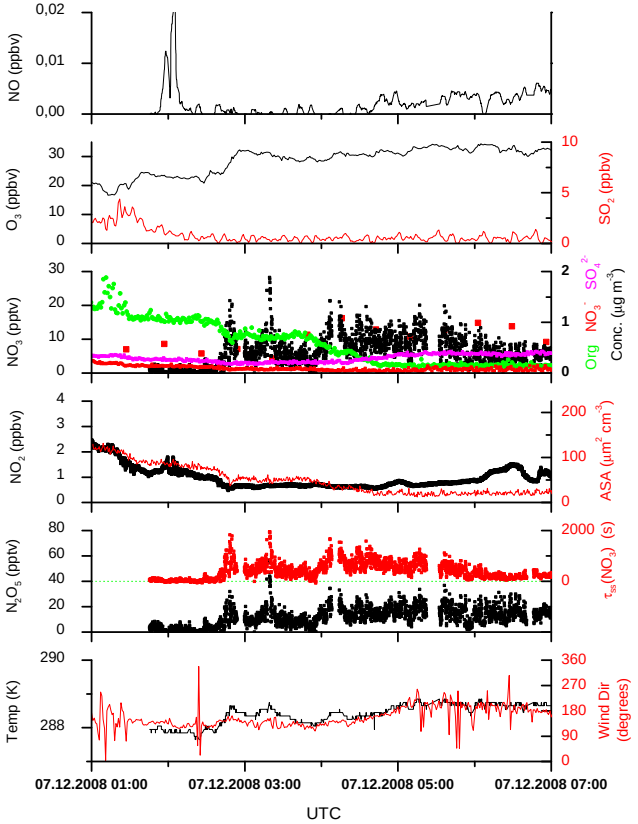


**Fig. 4.** Overview of measurements in the night of 6–7 December (air from the Atlantic sector). ASA = Aerosol surface area. For $NO_3$, the black dataponts are derived from CRD measurements of $N_2O_5$, the red squares are LP-DOAS measurements.





ACPD
11, 17825–17877, 2011



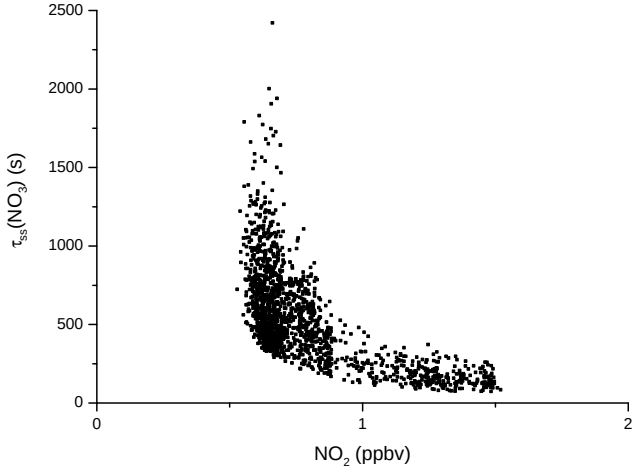


**Fig. 5.** Dependence of $NO_3$ lifetime, $\tau_{ss}(NO_3)$, on $NO_2$ mixing ratios (night of 6–7 December). The $NO_3$ lifetime was calculated using measurements of $N_2O_5$, $NO_2$ and $O_3$ (Eq. 1).





ACPD
11, 17825–17877, 2011



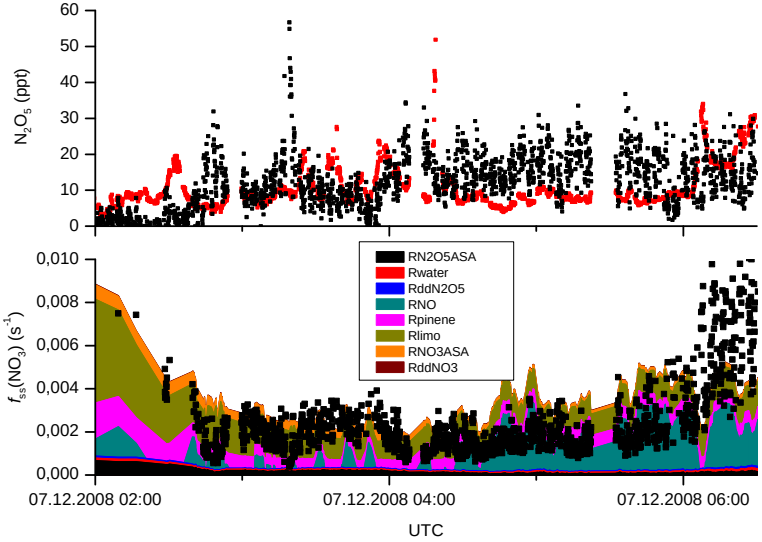


**Fig. 6.** Upper panel: Measured (black) and calculated (red) $N_2O_5$ mixing ratios in the night of 6–7 December. Steady-state $N_2O_5$ mixing ratios were calculated from the constrained production and loss terms for $NO_3$ and $N_2O_5$ and $K_2$ (Eq. 5). Lower Panel: Apportioned $NO_3$ loss rates over the same period. The various contributions are: RN2O5ASA = uptake of $N_2O_5$ to aerosol, Rwater = homogeneous hydrolysis of $N_2O_5$ with water vapour, RddN2O5 = dry deposition of $N_2O_5$, RNO = reaction of $NO_3$ with NO, Rpinene = reaction of $NO_3$ with $\alpha$-pinene, Rlimo = reaction of $NO_3$ with limonene, RNO3ASA = reaction of $NO_3$ on aerosol, RddNO3 = dry deposition of $NO_3$. The solid, black datapoints are measurements of the loss frequency of $NO_3$.





ACPD
11, 17825–17877, 2011



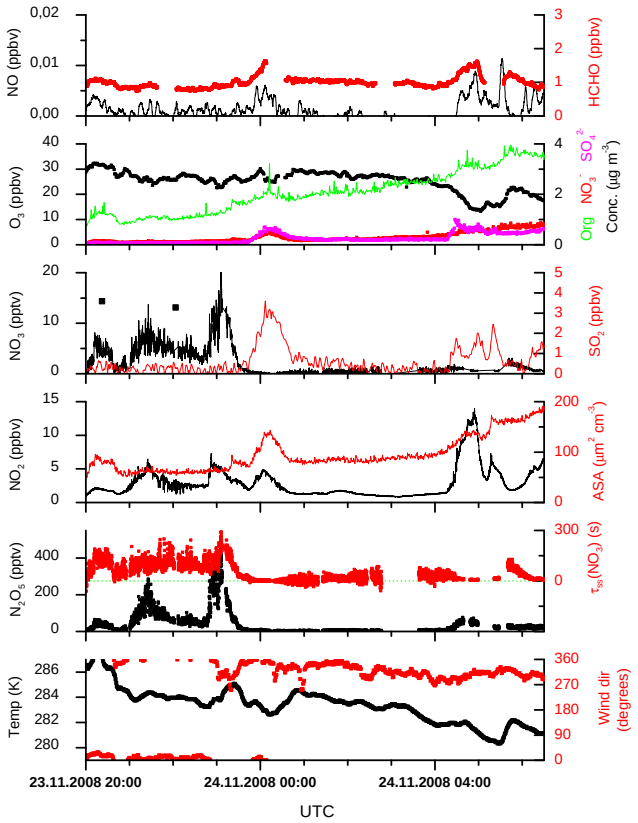


**Fig. 7.** Overview of measurements in the night of 23–24 in which the wind direction swung from the continental to Huelva sector. There were only very limited LP-DOAS measurements of NO3 on this night (black data points)





ACPD
11, 17825–17877, 2011



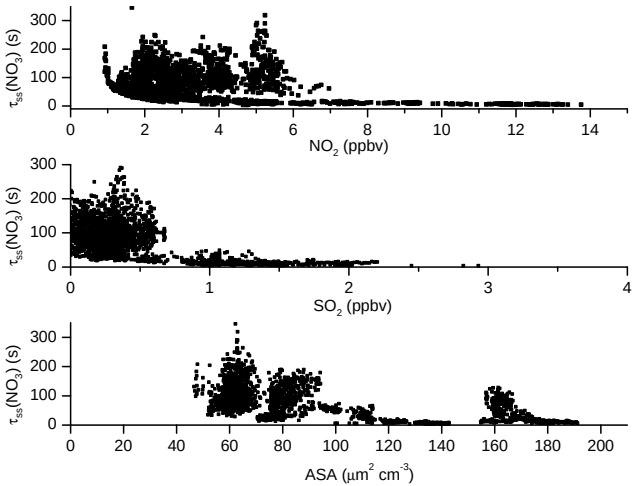


**Fig. 8.** 23–24 November: Dependence of $\tau_{ss}(NO_3)$ on $NO_2$ and $SO_2$ mixing ratios and the aerosol surface area (ASA). $\tau_{ss}(NO_3)$ was calculated using measurements of $N_2O_5$, $NO_2$ and $O_3$ (Eq. 1).





ACPD
11, 17825–17877, 2011



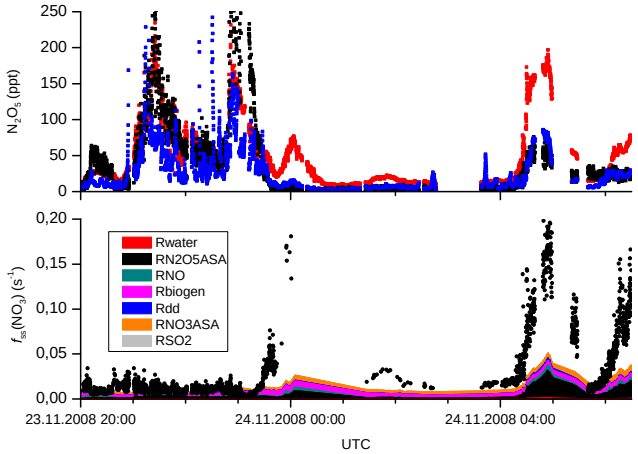


**Fig. 9.** Upper panel: Measured (black) and calculated (blue, red) $N_2O_5$ mixing ratios in the night of 23–24 November. Steady-state $N_2O_5$ mixing ratios were calculated from the constrained production and loss terms for $NO_3$ and $N_2O_5$ (E5). The red data points were calculated assuming no role of RSC, the blue data points include a $NO_3$ loss term related to $SO_2$ concentrations (see text). Lower panel: Apportioned $NO_3$ loss rates over the same period. The various contributions are: Rwater = homogeneous hydrolysis of $N_2O_5$ with water vapour, RN2O5ASA = uptake of $N_2O_5$ to aerosol, RNO = reaction of $NO_3$ with NO, Rbiogen = reaction of $NO_3$ with isoprene, limonene and $\alpha$-pinene, Rdd = summed dry deposition of $N_2O_5$ and $NO_3$, RNO3ASA = reaction of $NO_3$ on aerosol, RSO2 is the missing reactivity which has been scaled to correlate with $SO_2$ mixing ratios. The black dots datapoints are the calculated loss frequency of $NO_3$ (Eq. 1).





ACPD
11, 17825–17877, 2011



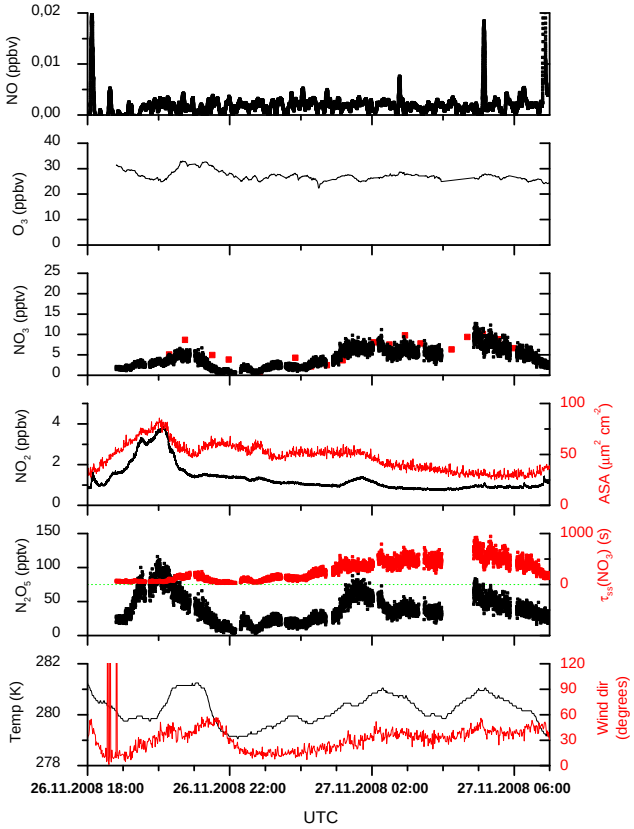


**Fig. 10.** Overview of measurements in the night 26–27 November (air from the continental sector). For $NO_3$, the black dataponts are CRD measurements, the red squares (~30 min resolution) are DOAS measurements.





ACPD
11, 17825–17877, 2011



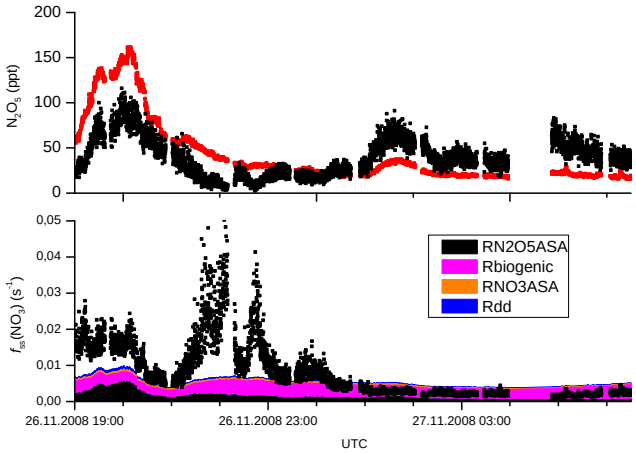


**Fig. 11.** Upper panel: Measured (black) and calculated (red) $N_2O_5$ mixing ratios in the night of 26–27 November. Steady-state $N_2O_5$ mising ratios were calculated from the constrained production and loss terms for $NO_3$ and $N_2O_5$ (E5). Lower panel: Apportioned $NO_3$ loss rates over the same period. The various contributions are: RN2O5ASA = uptake of $N_2O_5$ to aerosol (using $\gamma = 0.04$), Rbiogen = reaction of $NO_3$ with isoprene, limonene and $\alpha$-pinene, RNO3ASA = reaction of $NO_3$ on aerosol (using $\gamma = 0.1$), Rdd = summed dry deposition of $N_2O_5$ and $NO_3$. The black datapoints are measurements of loss frequency of $NO_3$.





ACPD
11, 17825–17877, 2011



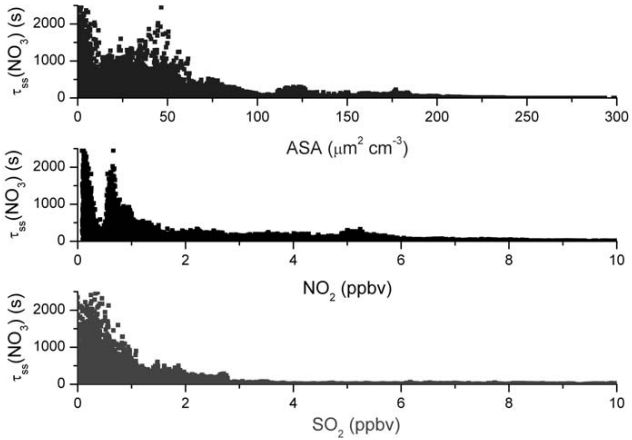


**Fig. 12.** Relationship between $NO_3$ lifetimes, $\tau_{ss}(NO_3)$ and the mixing ratios of $NO_2$, $SO_2$ and aerosol surface area (ASA) during the entire campaign.





ACPD
11, 17825–17877, 2011



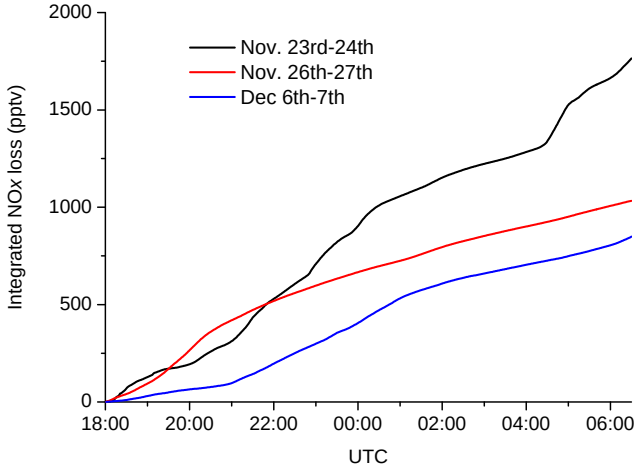


**Fig. 13.** Integrated loss of $NO_x$ on three campaign nights with air from the Huelva sector (black line), the continental sector (red line) and the Atlantic sector (blue line).





ACPD
11, 17825–17877, 2011